Resonant X-ray Photoelectron Spectroscopy: Identification of Atomic Contributions to Valence States

J. M. Seymour,[1] E. Gousseva,[1] R. A. Bennett,[1] A. I. Large,[2] G. Held,[2] D. Hein,[3] G. Wartner,[3] W. Quevedo,[3] R. Seidel,[3] C. Kolbeck,[4] C. J. Clarke,[5] R. M. Fogarty,[6] R. A. Bourne,[7] R. G. Palgrave,[8] P. A. Hunt,[9] K. R. J. Lovelock[1]

[1] Department of Chemistry, University of Reading, Reading, UK
[2] Diamond Light Source, Didcot, Oxfordshire, UK
[3] Helmholtz-Zentrum Berlin für Materialien und Energie (HZB), Berlin, Germany
[4] Fritz-Haber-Institut der Max-Planck-Gesellschaft, Berlin, Germany
[5] School of Chemistry, University of Nottingham, Nottingham, UK
[6] Department of Materials, Imperial College London, London, UK
[7] Institute of Process Research and Development, Schools of Chemistry and Chemical and Process Engineering, University of Leeds, Leeds, UK
[8] Department of Chemistry, University College London, London, UK
[9] School of Chemical and Physical Sciences, Victoria University of Wellington, Wellington, New Zealand

1. Samples Studied and Synthesis

Table S1 gives the samples studied.

The syntheses of $[C_8C_1Im]_2[CoCl_4]$ and $[C_8C_1Im]_2[Co(NTf_2)_4]$ were published in reference [1], the syntheses of $[C_8C_1Im][C(CN)_3]$, $[C_4C_1Im][SCN]$, $[P_{6,6,6,14}][NO_3]$, $[N_{2,1,1,0}][TfO]$ and $[N_{4,1,1,0}][HSO_4]$ were published in reference [2], and $[C_4C_1Im][BF_4]$ for lab XPS was purchased from Sigma-Aldrich. $[C_4C_1Im][BF_4]$ (for synchrotron XPS), $[C_4C_1Im]I$, $[C_4C_1Im][N(CN)_2]$, $[C_4C_1Im][SCN]$, $[C_4C_1Im][OAc]$, $[C_4C_1Im][TfO]$ were purchased from Iolitec. Three solvents (EtOH, MeCN and PC) were purchased from Sigma-Aldrich. Imidazole (purity >98%) was purchased from Iolitec. Highly demineralised water (conductivity ~0.2 μS cm^{-1}) was used for all aqueous samples.

Table S2 gives the samples studied by DFT calculations.

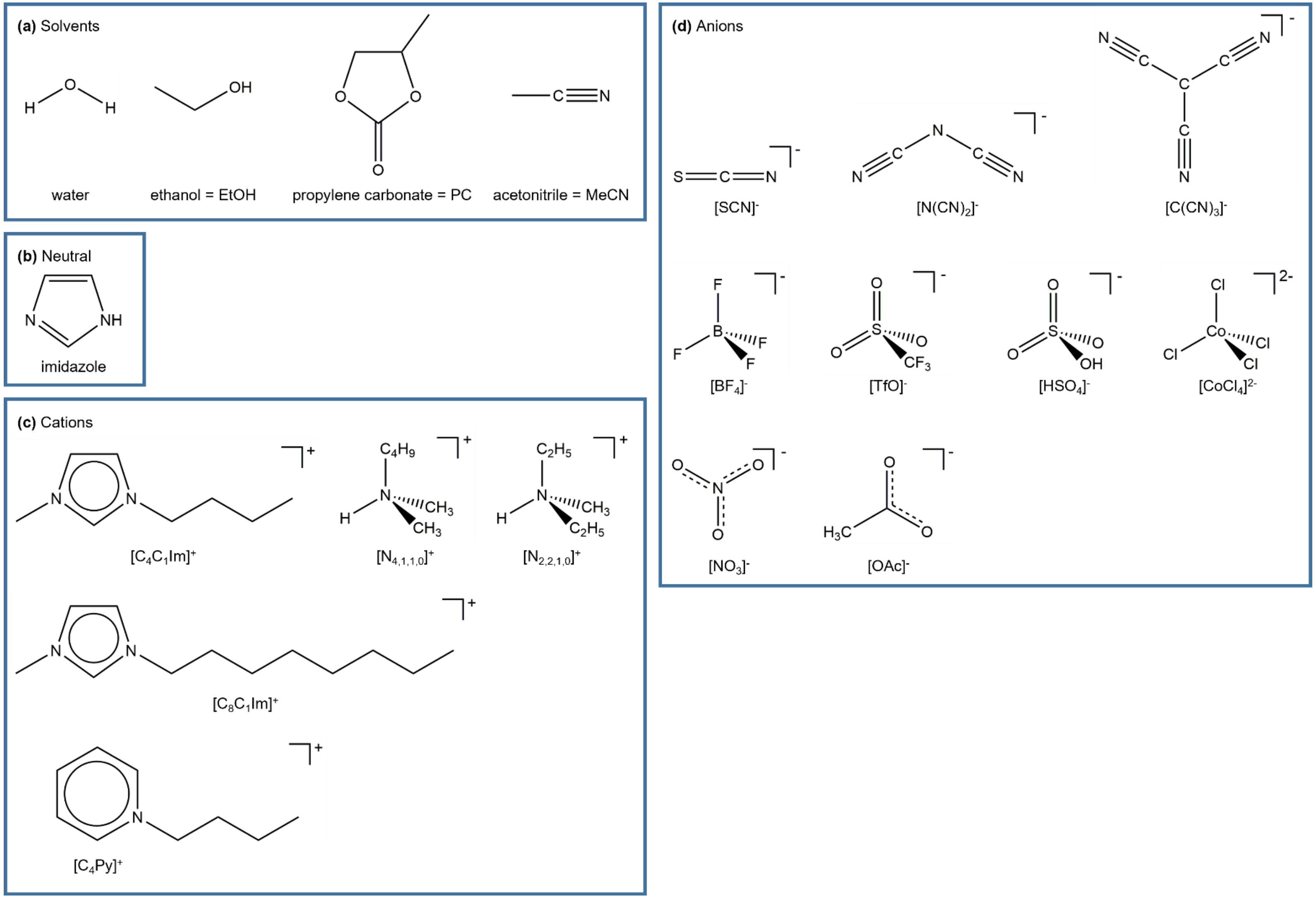

Figure S1. Polyatomic solvents/molecules/ions studied in this article: (a) solvents, (b) neutral molecule, (c) cations, (d) anions.

Table S1. Samples studied and apparatus used.

Solute	Solvent	Solute Concentration / M	RXPS Measured	Apparatus	Source-Electron Analyser Angle
	Water [a]		O 1s	U49/2-PGM 1, BESSY II	54.7°
	EtOH [b]		O 1s	U49/2-PGM 1, BESSY II	54.7°
	MeCN [c]		N 1s, C 1s	U49/2-PGM 1, BESSY II	54.7°
	PC [d]		O 1s, C 1s	U49/2-PGM 1, BESSY II	54.7°
Imidazole	Water	1.8	N 1s	U49/2-PGM 1, BESSY II	54.7°
K[SCN]	Water	0.5	C 1s	U49/2-PGM 1, BESSY II	54.7°
$[C_4C_1Im][BF_4]$	Water	0.5	F 1s, B 1s	U49/2-PGM 1, BESSY II	90.0°
$[C_4C_1Im]I$	Water	0.5	N 1s, C 1s	U49/2-PGM 1, BESSY II	90.0°
$[C_4C_1Im][N(CN)_2]$	Water	0.5	N 1s	U49/2-PGM 1, BESSY II	90.0°
$[C_4C_1Im][SCN]$	Water	0.5	N 1s	U49/2-PGM 1, BESSY II	90.0°
$[C_4C_1Im][OAc]$	Water	1.3	O 1s	U49/2-PGM 1, BESSY II	90.0°
$[C_4C_1Im][OAc]$	MeCN	0.5	O 1s	U49/2-PGM 1, BESSY II	90.0°
$[C_4C_1Im][TfO]$	Water	0.5	F 1s	U49/2-PGM 1, BESSY II	90.0°
$[N_{4,1,1,0}][HSO_4]$	Water	1.0	N 1s	U49/2-PGM 1, BESSY II	90.0°
$[N_{4,1,1,0}][HSO_4]$	Water	3.3	N 1s	U49/2-PGM 1, BESSY II	90.0°
not applicable	$[C_8C_1Im][C(CN)_3]$		N 1s	I311, MAX-lab	54.7°
not applicable	$[C_4C_1Im][SCN]$		N 1s	I311, MAX-lab	54.7°
not applicable	$[P_{6,6,6,14}][NO_3]$		O 1s, N 1s, C 1s	I311, MAX-lab	54.7°
not applicable	$[N_{2,2,1,0}][TfO]$		O 1s, N 1s, C 1s	I311, MAX-lab	54.7°
not applicable	$[N_{4,1,1,0}][HSO_4]$		O 1s, N 1s, C 1s	I311, MAX-lab	54.7°
not applicable	$[C_8C_1Im]_2[CoCl_4]$		Co $2p_{3/2}$	B07-C, DLS	54.7°
not applicable	$[C_8C_1Im]_2[Co(NTf_2)_4]$		C 1s	B07-C, DLS	54.7°
not applicable	$[C_4Py][NTf_2]$		N 1s	B07-C, DLS (ref. [1])	54.7°
not applicable	$[C_8C_1Im][SnCl_3]$		N 1s	I09, DLS (ref. [1])	80.0°
not applicable	$[C_4C_1Im][BF_4]$		not applicable	UCL (lab source)	54.7°

[a] Water: 20 mM NaCl

[b] EtOH: 20 mM NaCl

[c] MeCN: 50 mM NaI

[d] PC: 20 mM NaI

Table S2. Samples for which DFT calculations were carried out.

Species	SMD
[SCN]$^-$	[C_4C_1Im][PF_6]
[N(CN)$_2$]$^-$	[C_4C_1Im][PF_6]
[C(CN)$_3$]$^-$	[C_4C_1Im][PF_6]
[BF_4]$^-$	[C_4C_1Im][PF_6]
[TfO]$^-$	[C_4C_1Im][PF_6]
[NO_3]$^-$	[C_4C_1Im][PF_6]
[HSO_4]$^-$	[C_4C_1Im][PF_6]
[OAc]$^-$	[C_4C_1Im][PF_6]
[C_8C_1Im]$^+$	[C_4C_1Im][PF_6]
[$N_{4,1,1,0}$]$^+$	[C_4C_1Im][PF_6]
[$N_{2,2,1,0}$]$^+$	[C_4C_1Im][PF_6]
[C_4Py]$^+$	[C_4C_1Im][PF_6]
[$P_{6,6,6,14}$]$^+$	[C_4C_1Im][PF_6]
PC	PC
MeCN	MeCN
EtOH	EtOH
Water	Water
Imidazole	[C_4C_1Im][PF_6]

2. DFT calculations

2.1. SMD parameters

The SMD used for each lone molecule/ion is given in Table S2. For all ions (and neutral imidazole), whether solvated in ionic liquid or in molecular solvents, [C_4C_1Im][PF_6] SMD parameters were used for calculations (for consistency, Table S2). SMD parameters for solvent molecules (PC, MeCN, EtOH and water) were used (Table S2). [C_4C_1Im][PF_6] and PC values are as defined in Table S3, and the remaining solvent parameters employed the defaults within Gaussian 16. The relative permittivity is reported for all solvents for comparison.

Table S3. Parameters used in the SMD model and the references used to obtain the parameters.

Solvent	Relative permittivity, ε_r	Refractive index, *n*	Surface tension, γ/ cal mol^{-1} Å^2)	Abraham acidity, *α*	Abraham basicity, *β*
[C_4C_1Im][PF_6]	11.40 [3]	1.4090 [3]	70.24 [3]	0.266 [3]	0.216 [3]
Water	78.36	internal	internal	internal	internal
MeCN	35.69	internal	internal	internal	internal
EtOH	24.85	internal	internal	internal	internal
PC	66.14 [4, 5]	2.013 [6]	59.00 [7]	0.00 [8]	0.64 [8]

2.2. DoS, pDoS and Gelius-weighted DoS

All density of states (DoS), partial DoS (pDoS) and Gelius-weighted DoS were generated for the lowest energy conformer for each system. The DoS of a system is defined as follows.

2.2.1. DoS

$$DoS(E_B) = \sum_i F(E_B - (-\xi_i))$$

where *F* is a broadening function and E_B is binding energy (the negative of energy, positive binding energies indicate stable states). A GL30 (70% Gaussian, 30% Lorentzian) broadening function (with full width at half maximum, FWHM, dependent on the data set) was used for all DoS plots.

2.2.2. Gaussian-Lorentzian broadening

The exact form of the broadening function (referred to as GL30) used in pDoS is shown below (along with the formula for the DoS).

$$DoS(E_B) = \sum_i F(E_B - (-\xi_i))$$

$$F(E_B - (-\xi_i)) = 0.7G(E_B - (-\xi_i)) + 0.3L(E_B - (-\xi_i))$$

$$G(E_B - (-\xi_i)) = \frac{1}{\eta\sqrt{2\pi}}exp(\frac{-(E_B - (-\xi_i))^2}{2\eta^2})$$

$$L(E_B - (-\xi_i)) = \frac{1}{\pi}\frac{0.5\Gamma}{(E_B - (-\xi_i))^2 + 0.5\Gamma^2}$$

$$\Gamma = FWHM$$

$$\eta = \frac{\Gamma}{2\sqrt{2ln2}}$$

A broadening function (FWHM = 1.0 eV) was used for all calculated DoS.

2.2.3. pDoS

The pDoS of an atomic orbital *k* is defined as:

$$pDoS(k, E_B) = \sum_i n_{k,i}F(E_B - (-\xi_i))$$

where $n_{k,i}$ is the fractional contribution of AO *k* to MO *i*. The value of $n_{\mathrm{k,i}}$ was determined using Mulliken population analysis as implemented in multiwfn.[9,10] The pDOS for a fragment (*e.g*. the nitrogen in $[SCN]^-$) was obtained by summing the pDoS for all AOs centred on that fragment.

2.3. Generating Conformers

DFT calculations were carried out using Becke's three–parameter exchange functional in combination with the Lee, Yang and Parr correlation functional (B3LYP) as implemented in the Gaussian 09 and Gaussian 16 suite of programs.[11-13] Grimme's D3 dispersion correction with Becke–Johnson damping was used to account for dispersion.[14-17] The combination of B3LYP with D3–BJ damping is referred to as the B3LYP–D3(BJ) functional henceforth. The 6–311+G(d,p) basis set was employed for all calculations.

Optimisations were carried out under no symmetry constraints. The SCF convergence criteria were tightened from the Gaussian 09 defaults to 10^{-9} on the density matrix and 10^{-7} on the energy matrix. The numerical integration grid was improved from the Gaussian 09 defaults to a pruned grid with 99 radial shells and 590 angular points per shell. All structures were proved to be minima via confirmation that all vibrational frequencies are positive.

3. Explanation of spectator Auger transitions

- Step 1 for spectator Auger emission: X-ray absorption (Figure 1c).
- Step 2 for spectator Auger emission: an electron from an occupied core/valence state refills the core-hole and an electron from an occupied core/valence state is ejected; the electron excited during X-ray absorption remains in the previously unoccupied valence state, spectating on the Auger emission process (Figure 1e). The process closely resembles normal Auger emission, but with the spectator electron in place. The final state for SA emission is 2h1e$_u$ (with the two hole either core or valence, Figure 1e).

4. RXPS maps: solvents

4.1. RXPS maps: water

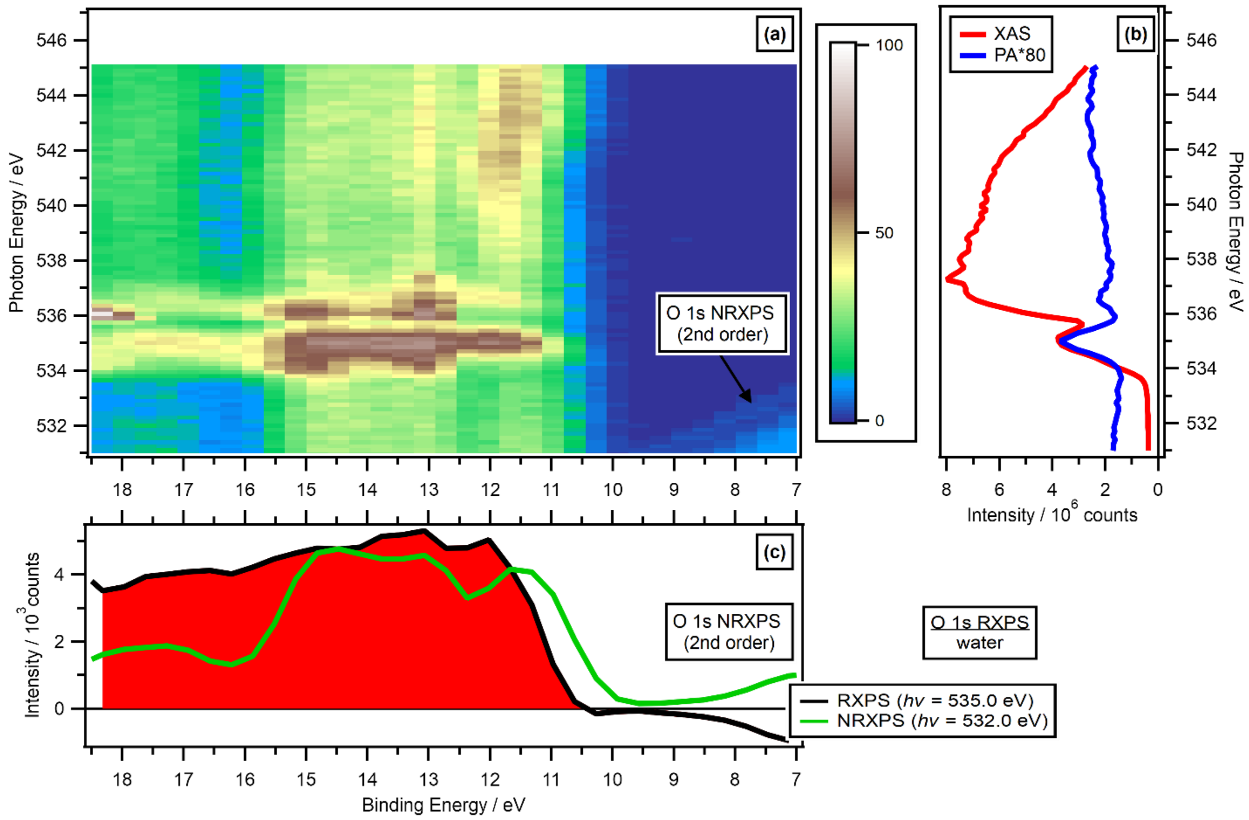

Figure S2. O 1s valence RXPS for water (plus 20 mM NaCl). (a) O 1s valence RXPS heat map for water. (b) Partial electron yield O 1s NEXAFS spectra (spectator Auger region plus participator Auger region = XAS, and participator Auger region only). (c) O 1s valence NRXP spectrum ($h\nu$ = 532.0 eV) and O 1s valence RXP spectrum ($h\nu$ = 535.0 eV, with the valence NRXPS contributions subtracted; estimated participator Auger contribution shaded red). The valence NRXPS contributions were subtracted using the procedure outlined in reference [2]. All valence XP spectra were charge referenced using procedures outlined in Section 2.5.

4.2. RXPS maps: EtOH

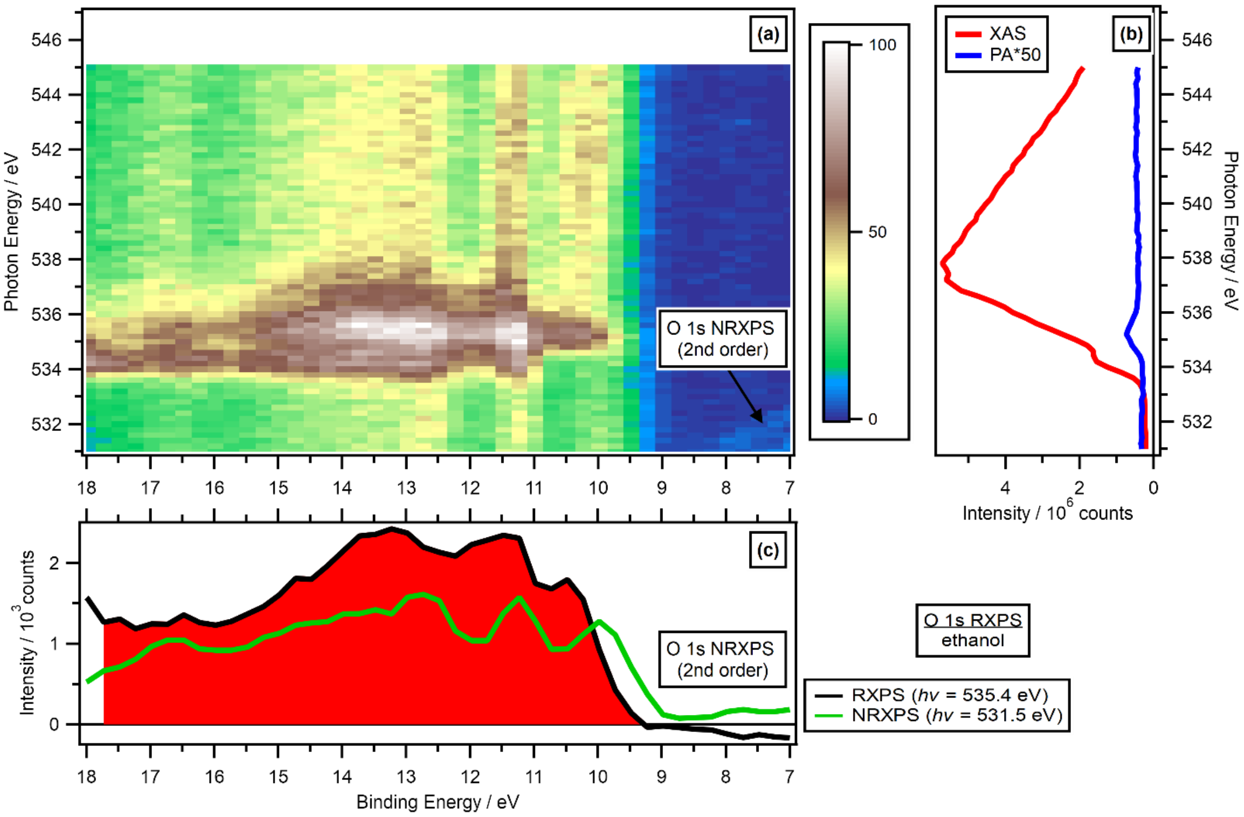

Figure S3. O 1s RXPS for EtOH (plus 20 mM NaCl). (a) O 1s valence RXPS heat map for EtOH. (b) Partial electron yield O 1s NEXAFS spectra (spectator Auger region plus participator Auger region = XAS, and participator Auger region only). (c) O 1s valence NRXP spectrum ($h\nu$ = 531.5 eV) and O 1s valence RXP spectrum ($h\nu$ = 535.4 eV, with the valence NRXPS contributions subtracted; estimated participator Auger contribution shaded red). The valence NRXPS contributions were subtracted using the procedure outlined in reference [2]. All valence XP spectra were charge referenced using procedures outlined in Section 2.5.

4.3. RXPS maps: PC

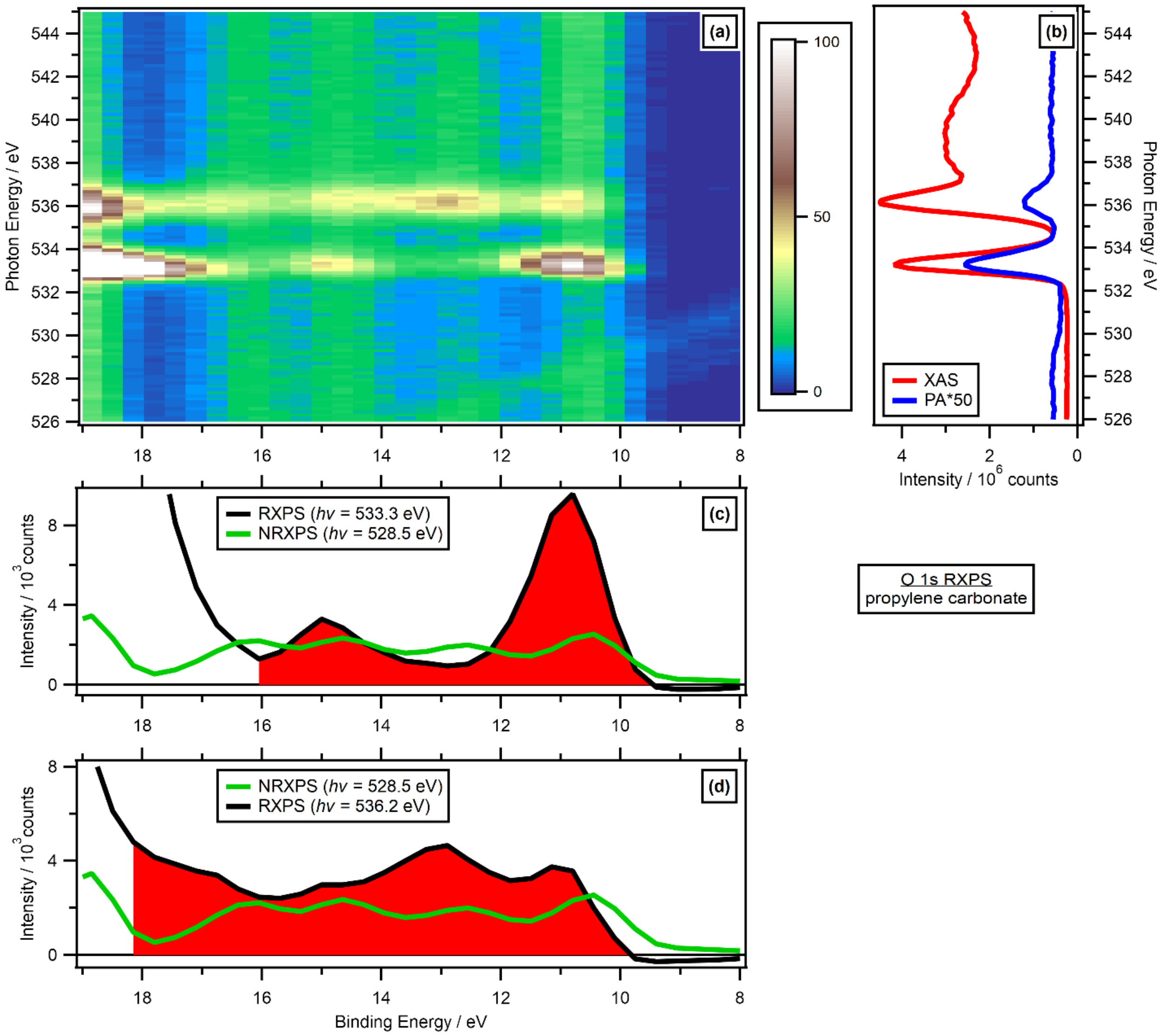

Figure S4. O 1s RXPS for PC (plus 20 mM NaI). (a) O 1s valence RXPS heat map for PC. (b) Partial electron yield O 1s NEXAFS spectra (spectator Auger region plus participator Auger region = XAS, and participator Auger region only). (c) O 1s valence NRXP spectrum ($h\nu$ = 528.5 eV) and O 1s valence RXP spectrum ($h\nu$ = 533.3 eV, with the valence NRXPS contributions subtracted; estimated participator Auger contribution shaded red). (d) O 1s valence NRXP spectrum ($h\nu$ = 528.5 eV) and O 1s valence RXP spectrum ($h\nu$ = 536.2 eV, with the valence NRXPS contributions subtracted; estimated participator Auger contribution shaded red). The NRXPS contributions were subtracted using the procedure outlined in reference [2]. All electron spectra were charge referenced using procedures outlined in Section 2.5.

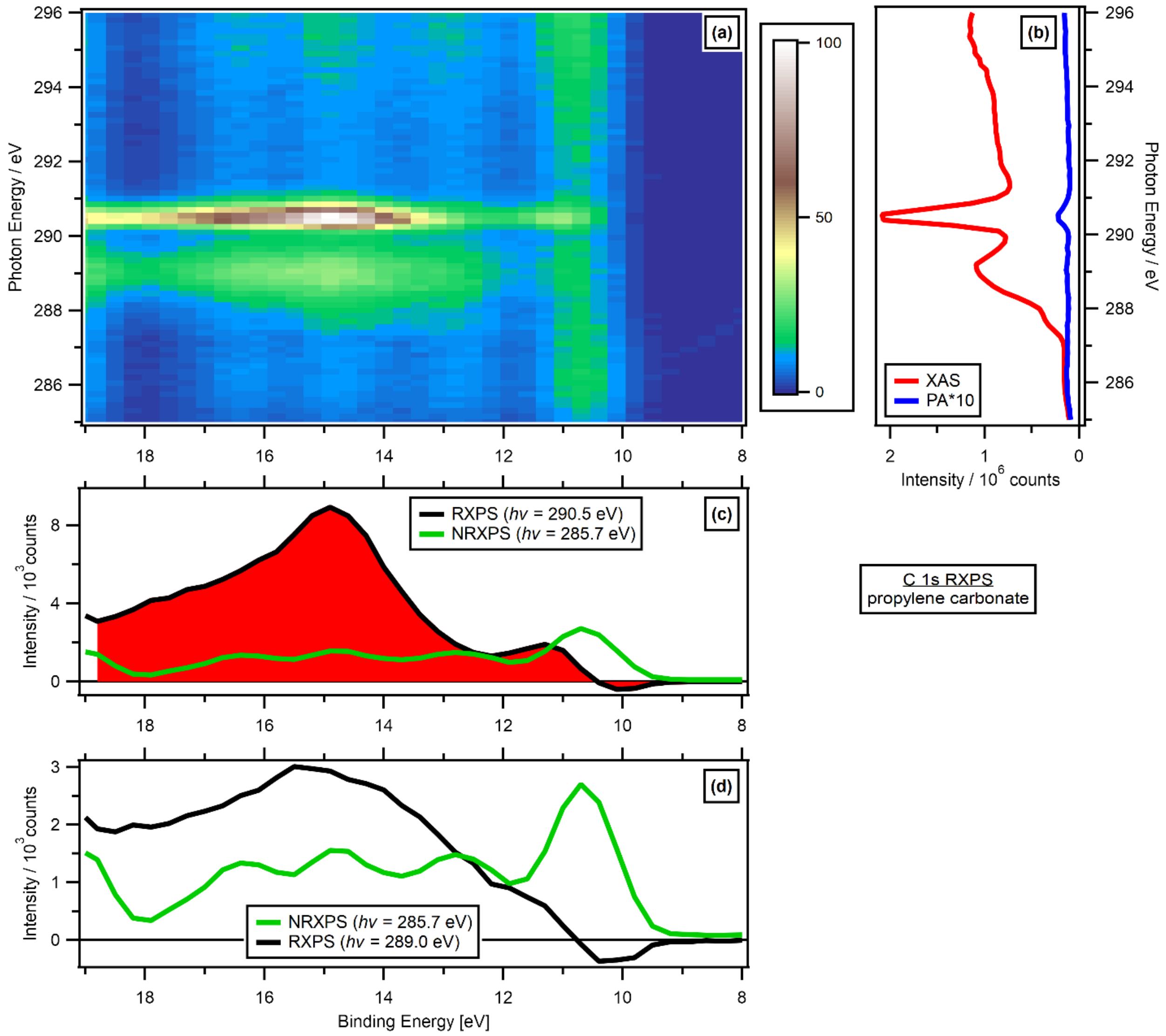

Figure S5. C 1s RXPS for PC (plus 20 mM NaI). (a) C 1s valence RXPS heat map for PC. (b) Partial electron yield C 1s NEXAFS spectra (spectator Auger region plus participator Auger region = XAS, and participator Auger region only). (c) C 1s valence NRXP spectrum ($h\nu$ = 285.7 eV) and C 1s valence RXP spectrum ($h\nu$ = 290.5 eV, with the valence NRXPS contributions subtracted; estimated participator Auger contribution shaded red). (d) C 1s valence NRXP spectrum ($h\nu$ = 285.7 eV) and C 1s valence RXP spectrum ($h\nu$ = 289.0 eV, with the valence NRXPS contributions subtracted; estimated participator Auger contribution shaded red). The NRXPS contributions were subtracted using the procedure outlined in reference [2]. All electron spectra were charge referenced using procedures outlined in Section 2.5.

4.4. RXPS maps: MeCN

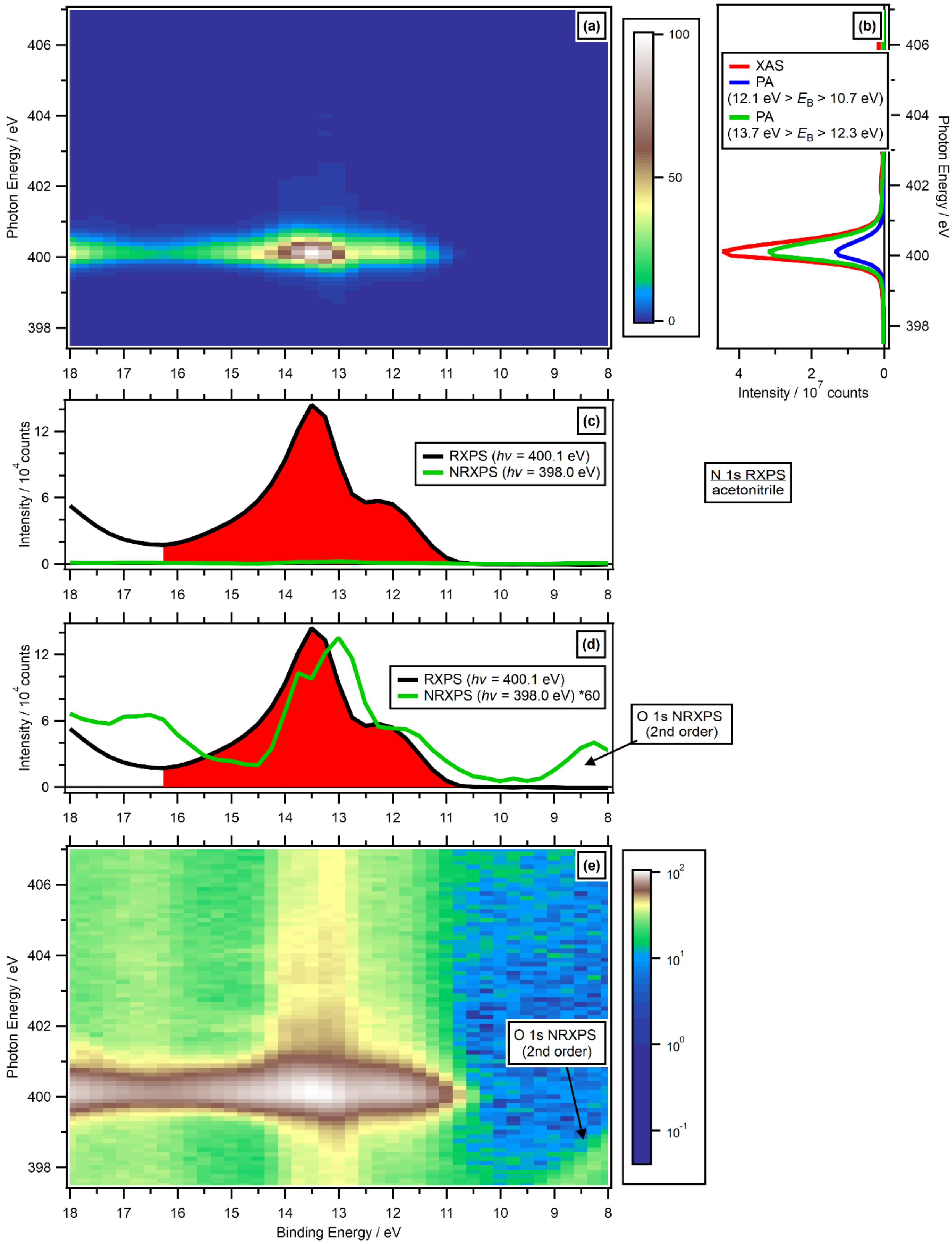

Figure S6. N 1s RXPS for MeCN (plus 50 mM NaI). (a) N 1s valence RXPS heat map for MeCN. (b) Partial electron yield N 1s NEXAFS spectra (spectator Auger region plus participator Auger region = XAS, and participator Auger regions only). (c) N 1s valence NRXP spectrum ($h\nu$ = 398.0 eV) and N 1s valence RXP spectrum ($h\nu$ = 400.1 eV, with the valence NRXPS contributions subtracted; estimated participator Auger contribution shaded red). (d) Same as (c), but with the NRXPS multiplied by 60. (e) N 1s valence RXPS heat map for MeCN, plotted on a log y-scale. The NRXPS contributions were subtracted using the procedure outlined in reference [2]. All electron spectra were charge referenced using procedures outlined in Section 2.5.

4.5. RXPS maps: $[C_8C_1Im]_2[CoCl_4]$

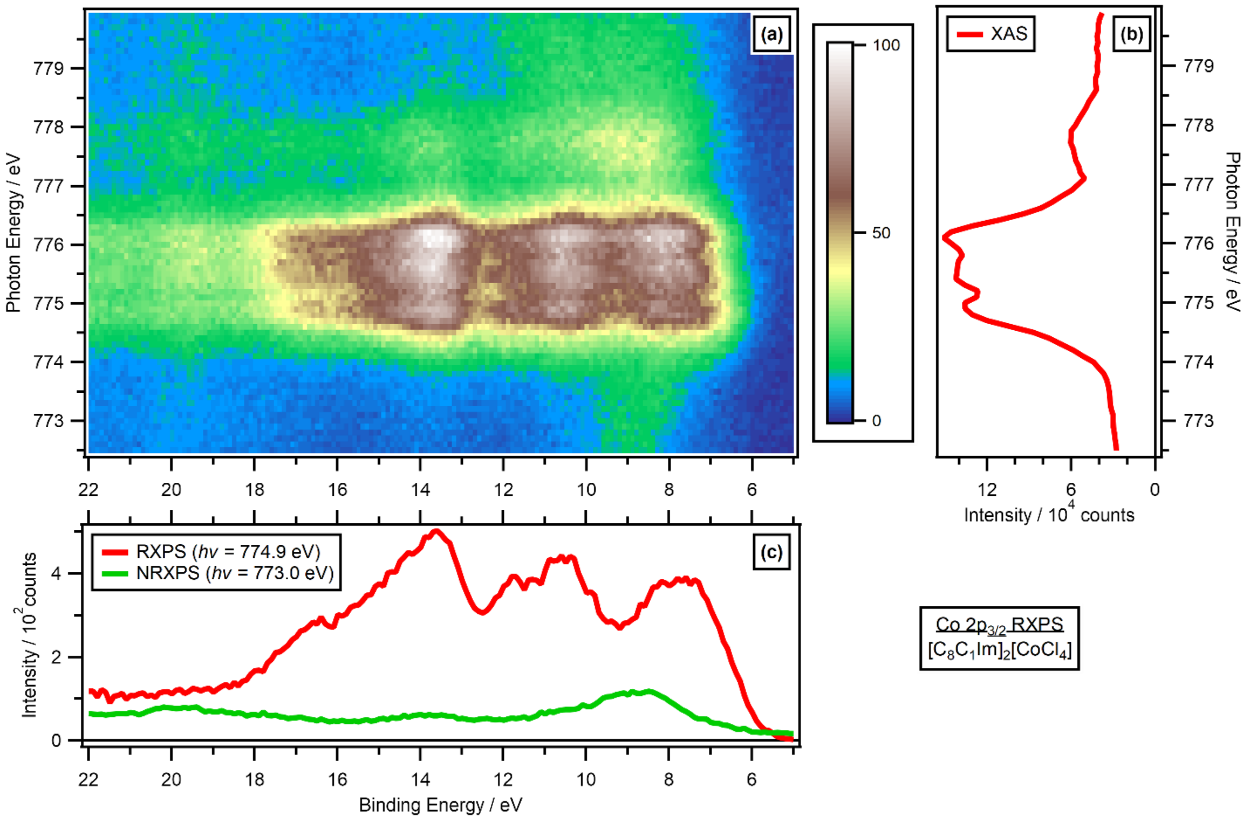

Figure S7. Co $2p_{3/2}$ RXPS for $[C_8C_1Im]_2[CoCl_4]$. (a) Co $2p_{3/2}$ valence RXPS heat map for $[C_8C_1Im]_2[CoCl_4]$. (b) Partial electron yield Co $2p_{3/2}$ NEXAFS spectra. (c) Co $2p_{3/2}$ valence NRXP spectrum ($h\nu$ = 773.0 eV) and Co $2p_{3/2}$ valence RXP spectrum ($h\nu$ = 774.9 eV, with the valence NRXPS contributions subtracted. The NRXPS contributions were subtracted using the procedure outlined in reference [2]. All electron spectra were charge referenced using procedures outlined in Section 2.5.

4.6. RXPS maps: $[C_8C_1Im][C(CN)_3]$

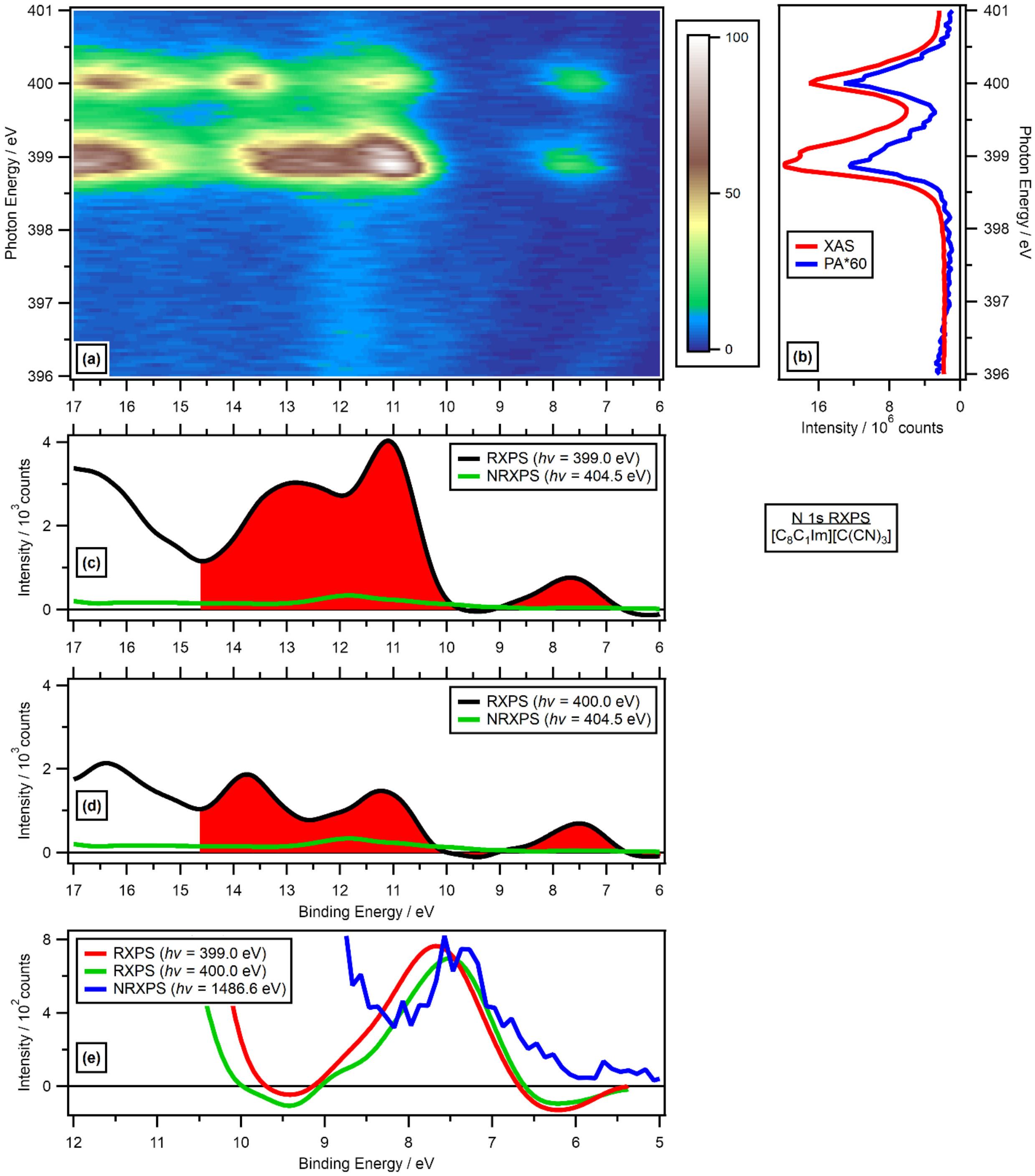

Figure S8. N 1s RXPS for $[C_8C_1Im][C(CN)_3]$. (a) N 1s valence RXPS heat map for $[C_8C_1Im][C(CN)_3]$. (b) Partial electron yield N 1s NEXAFS spectra (spectator Auger region plus participator Auger region = XAS, and participator Auger regions only). (c) N 1s valence NRXP spectrum ($h\nu$ = 404.5 eV) and N 1s valence RXP spectrum ($h\nu$ = 399.0 eV, with the valence NRXPS contributions subtracted; estimated participator Auger contribution shaded red). (d) N 1s valence NRXP spectrum ($h\nu$ = 404.5 eV) and N 1s valence RXP spectrum ($h\nu$ = 400.0 eV, with the valence NRXPS contributions subtracted; estimated participator Auger contribution shaded red). (e) N 1s valence NRXP spectrum ($h\nu$ = 1486.6 eV) and N 1s valence RXP spectra ($h\nu$ = 399.0 eV and $h\nu$ = 400.0 eV, with the valence NRXPS contributions subtracted). The NRXPS contributions were subtracted using the procedure outlined in reference [2]. All electron spectra were charge referenced using procedures outlined in Section 2.5.

4.7. RXPS maps: other ILs

RXPS maps for five ionic liquids ($[C_8C_1Im][C(CN)_3]$, $[C_4C_1Im][SCN]$, $[P_{6,6,6,14}][NO_3]$, $[N_{2,1,1,0}][TfO]$, $[N_{4,1,1,0}][HSO_4]$) were published in reference [2]. RXPS maps for three ionic liquids ($[C_8C_1Im]_2[Co(NTf_2)_4]$, $[C_4Py][NTf_2]$, $[C_8C_1Im][SnCl_3]$) were published in reference [1].

5. RXPS maps: solutes

5.1. RXPS maps: 1.8 M imidazole in water

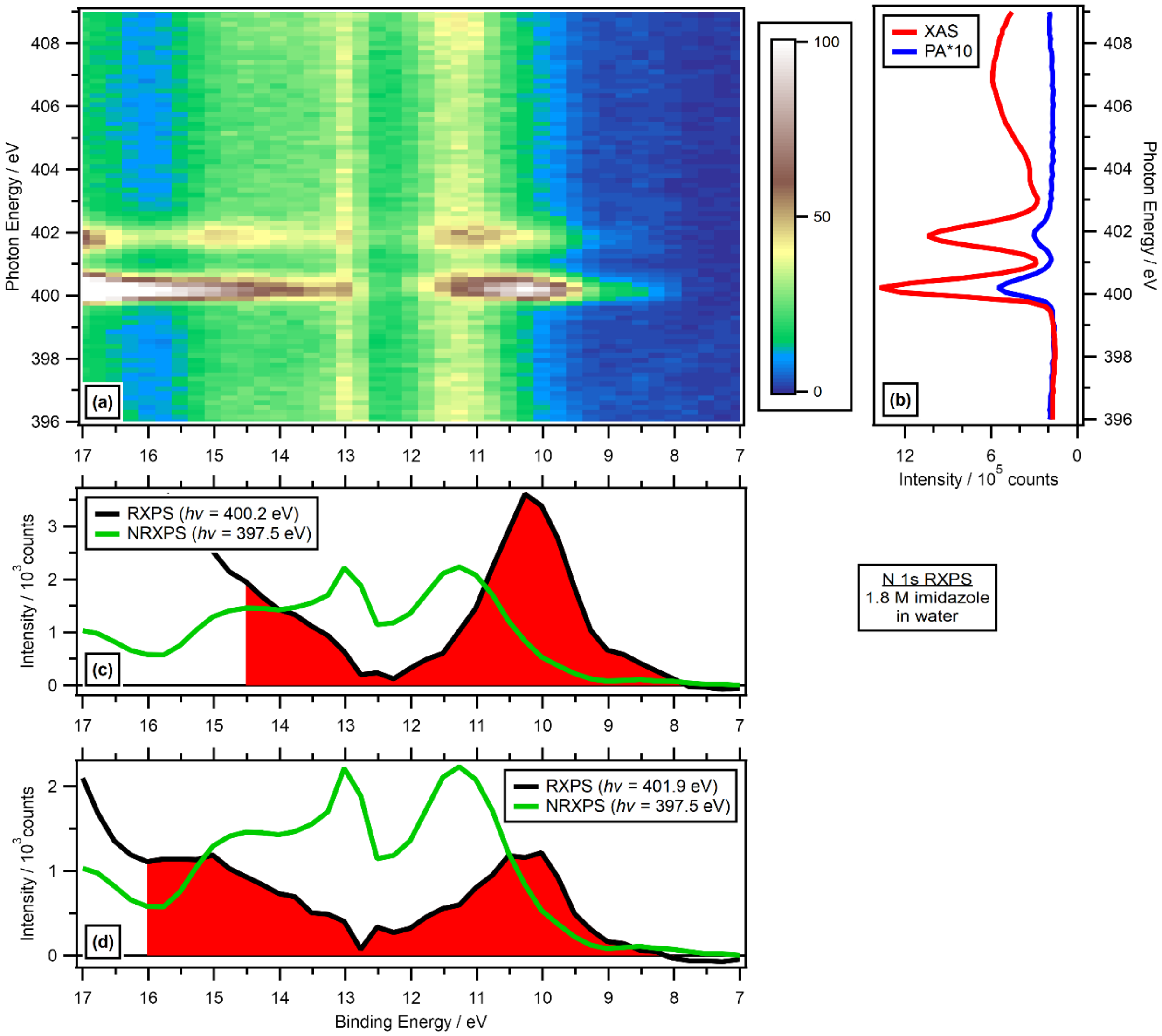

Figure S9 N 1s RXPS for 1.8 M imidazole in water (plus 20 mM NaCl). (a) N 1s valence RXPS heat map for 1.8 M imidazole in water. (b) Partial electron yield N 1s NEXAFS spectra (spectator Auger region plus participator Auger region = XAS, and participator Auger region only). (c) N 1s valence NRXP spectrum ($h\nu$ = 397.5 eV) and N 1s valence RXP spectrum ($h\nu$ = 400.2 eV, with the valence NRXPS contributions subtracted; estimated participator Auger contribution shaded red). (d) N 1s valence NRXP spectrum ($h\nu$ = 397.5 eV) and N 1s valence RXP spectrum ($h\nu$ = 401.9 eV, with the valence NRXPS contributions subtracted; estimated participator Auger contribution shaded red). The NRXPS contributions were subtracted using the procedure outlined in reference [2]. All electron spectra were charge referenced using procedures outlined in Section 2.5.

5.2. RXPS maps: 0.5 M KSCN in water

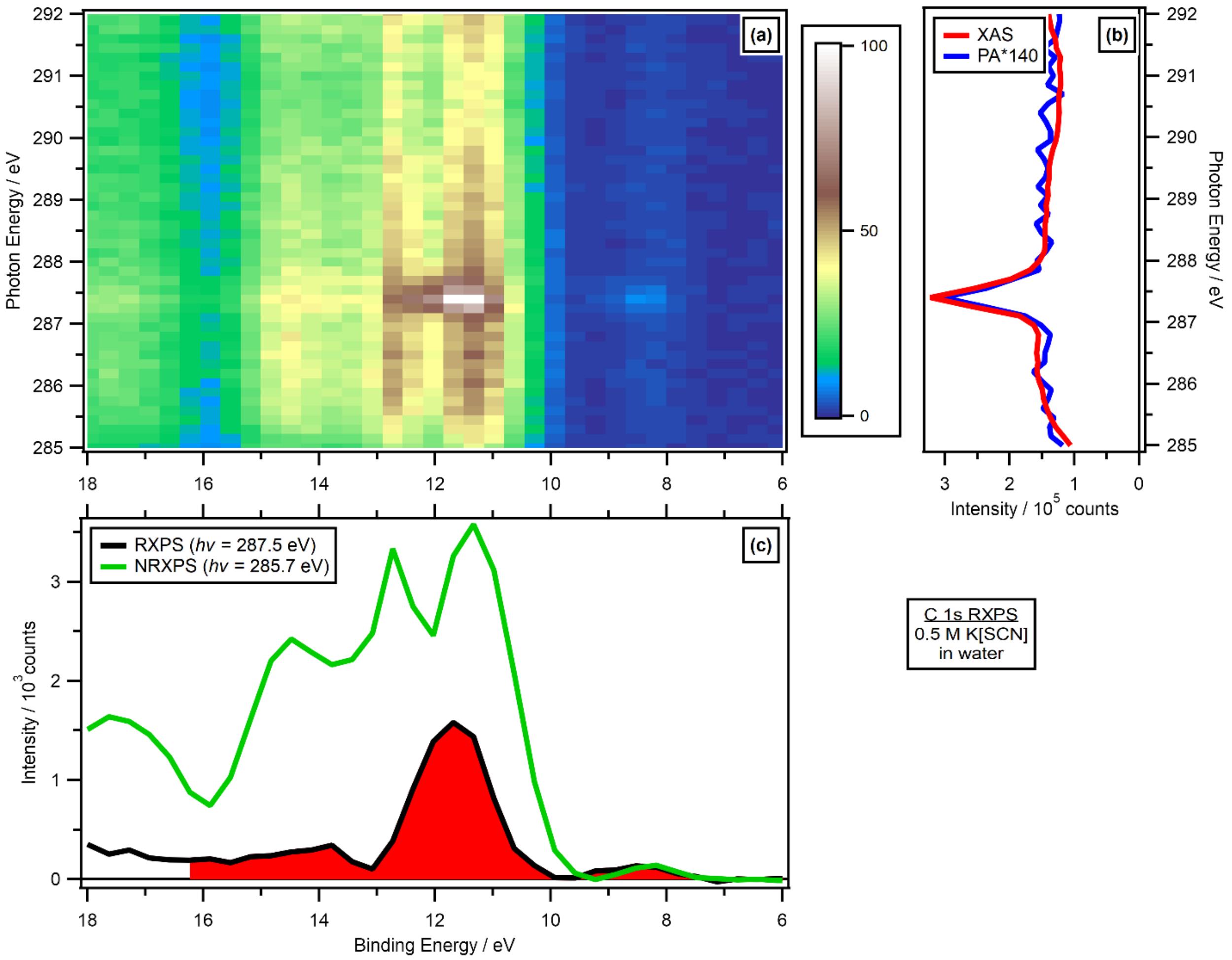

Figure S10. C 1s RXPS for 0.5 M K[SCN] in water. (a) C 1s valence RXPS heat map for 0.5 M K[SCN] in water. (b) Partial electron yield C 1s NEXAFS spectra (spectator Auger region plus participator Auger region = XAS, and participator Auger region only). (c) C 1s valence NRXP spectrum ($h\nu$ = 285.7 eV) and C 1s valence RXP spectrum ($h\nu$ = 287.5 eV, with the valence NRXPS contributions subtracted; estimated participator Auger contribution shaded red). The NRXPS contributions were subtracted using the procedure outlined in reference [2]. All electron spectra were charge referenced using procedures outlined in Section 2.5.

5.3. RXPS maps: 0.5 M $[C_4C_1Im][BF_4]$ in water

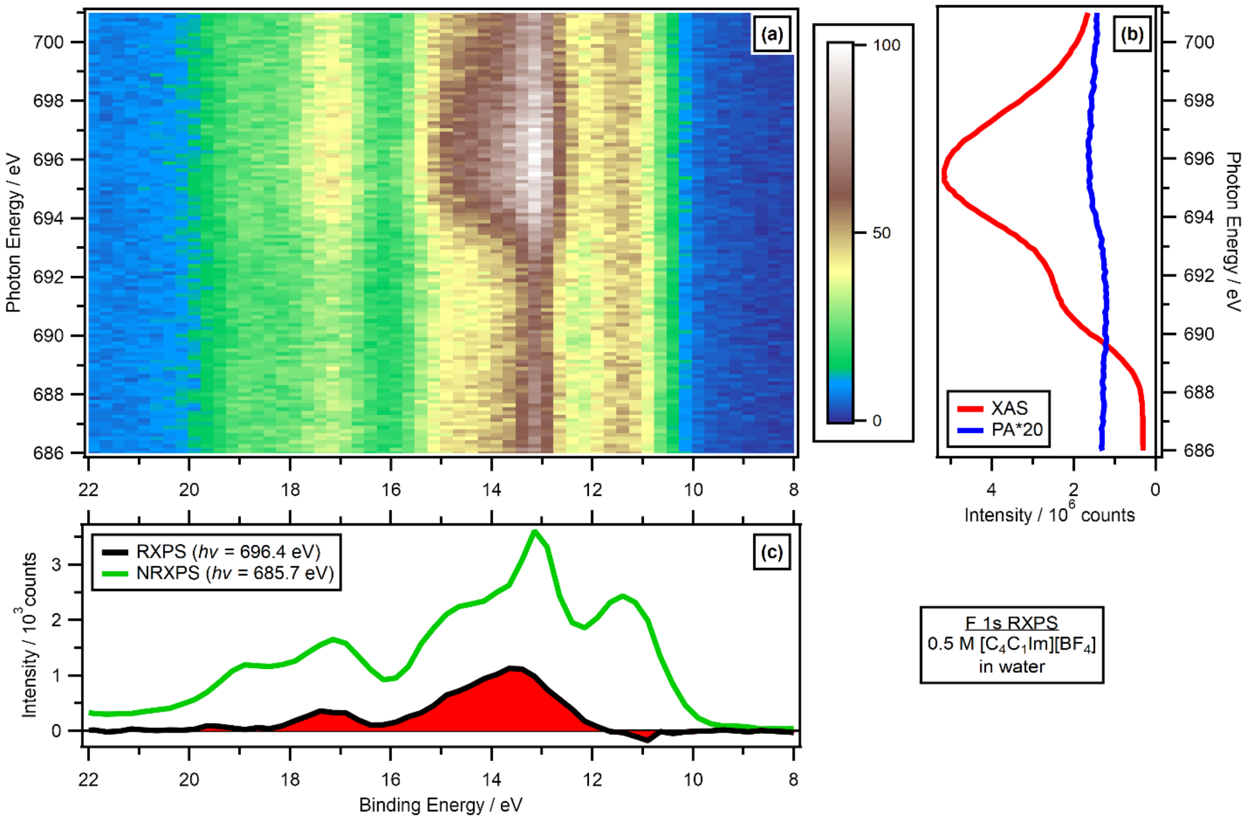

Figure S11. F 1s RXPS for 0.5 M $[C_4C_1Im][BF_4]$ in water. (a) F 1s valence RXPS heat map for 0.5 M $[C_4C_1Im][BF_4]$ in water. (b) Partial electron yield F 1s NEXAFS spectra (spectator Auger region plus participator Auger region = XAS, and participator Auger region only). (c) F 1s valence NRXP spectrum ($h\nu$ = 685.7 eV) and F 1s valence RXP spectrum ($h\nu$ = 696.4 eV, with the valence NRXPS contributions subtracted; estimated participator Auger contribution shaded red). The NRXPS contributions were subtracted using the procedure outlined in reference [2]. All electron spectra were charge referenced using procedures outlined in Section 2.5.

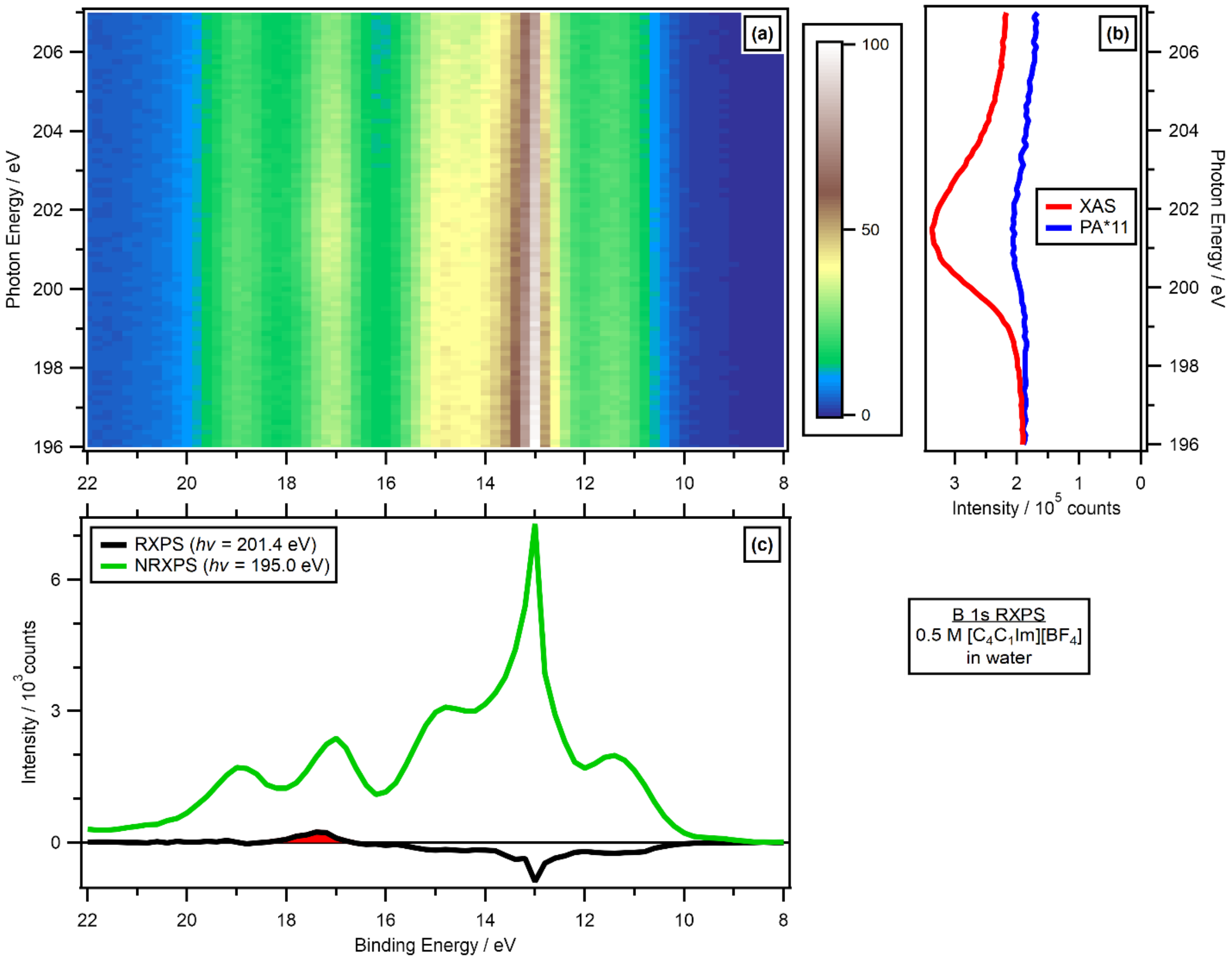

Figure S12. B 1s RXPS for 0.5 M $[C_4C_1Im][BF_4]$ in water. (a) B 1s valence RXPS heat map for 0.5 M $[C_4C_1Im][BF_4]$ in water. (b) Partial electron yield B 1s NEXAFS spectra (spectator Auger region plus participator Auger region = XAS, and participator Auger region only). (c) B 1s valence NRXP spectrum ($h\nu$ = 195.0 eV) and B 1s valence RXP spectrum ($h\nu$ = 201.4 eV, with the valence NRXPS contributions subtracted; estimated participator Auger contribution shaded red). The NRXPS contributions were subtracted using the procedure outlined in reference [2]. All electron spectra were charge referenced using procedures outlined in Section 2.5.

5.4. RXPS maps: 0.5 M [C_4C_1Im]I in water

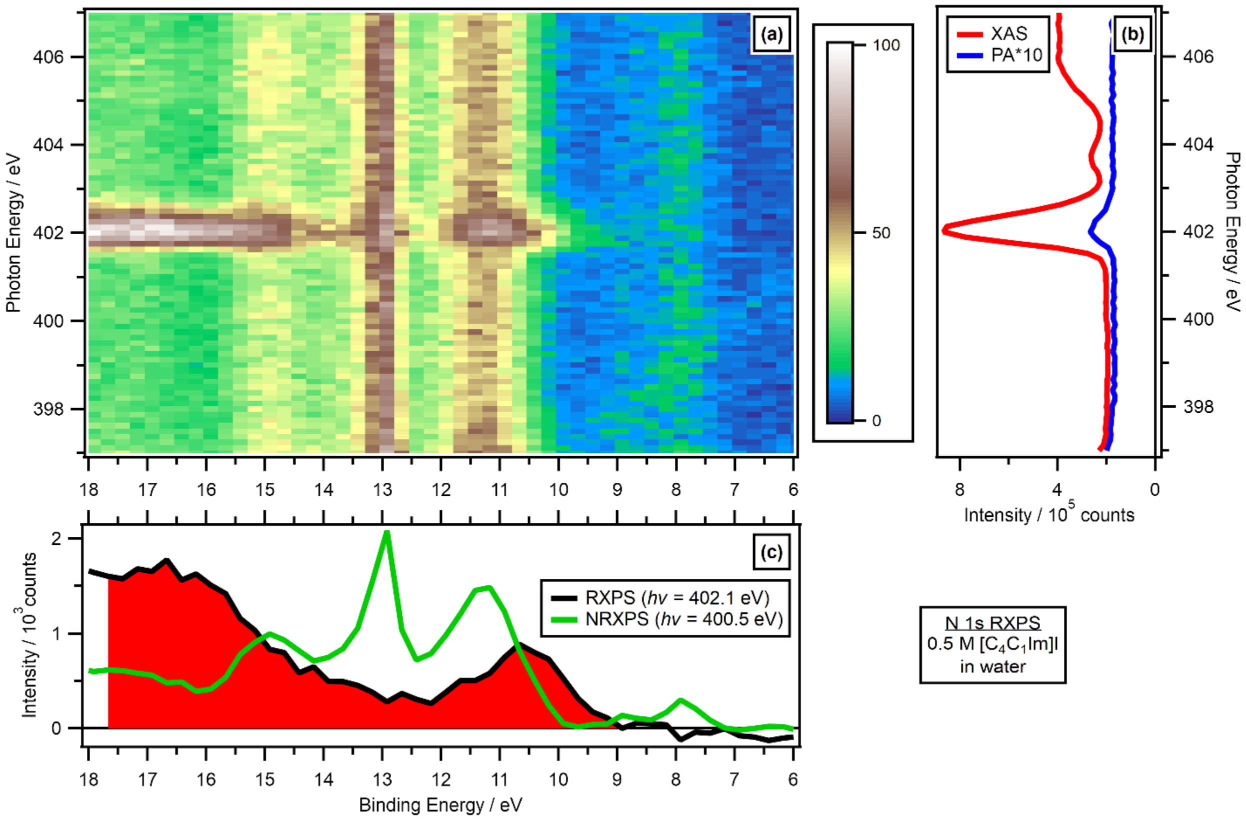

Figure S13. N 1s RXPS for 0.5 M [C_4C_1Im]I in water. (a) N 1s valence RXPS heat map for 0.5 M [C_4C_1Im]I in water. (b) Partial electron yield N 1s NEXAFS spectra (spectator Auger region plus participator Auger region = XAS, and participator Auger region only). (c) N 1s valence NRXP spectrum ($h\nu$ = 400.5 eV) and N 1s valence RXP spectrum ($h\nu$ = 402.1 eV, with the valence NRXPS contributions subtracted; estimated participator Auger contribution shaded red). The NRXPS contributions were subtracted using the procedure outlined in reference [2]. All electron spectra were charge referenced using procedures outlined in Section 2.5.

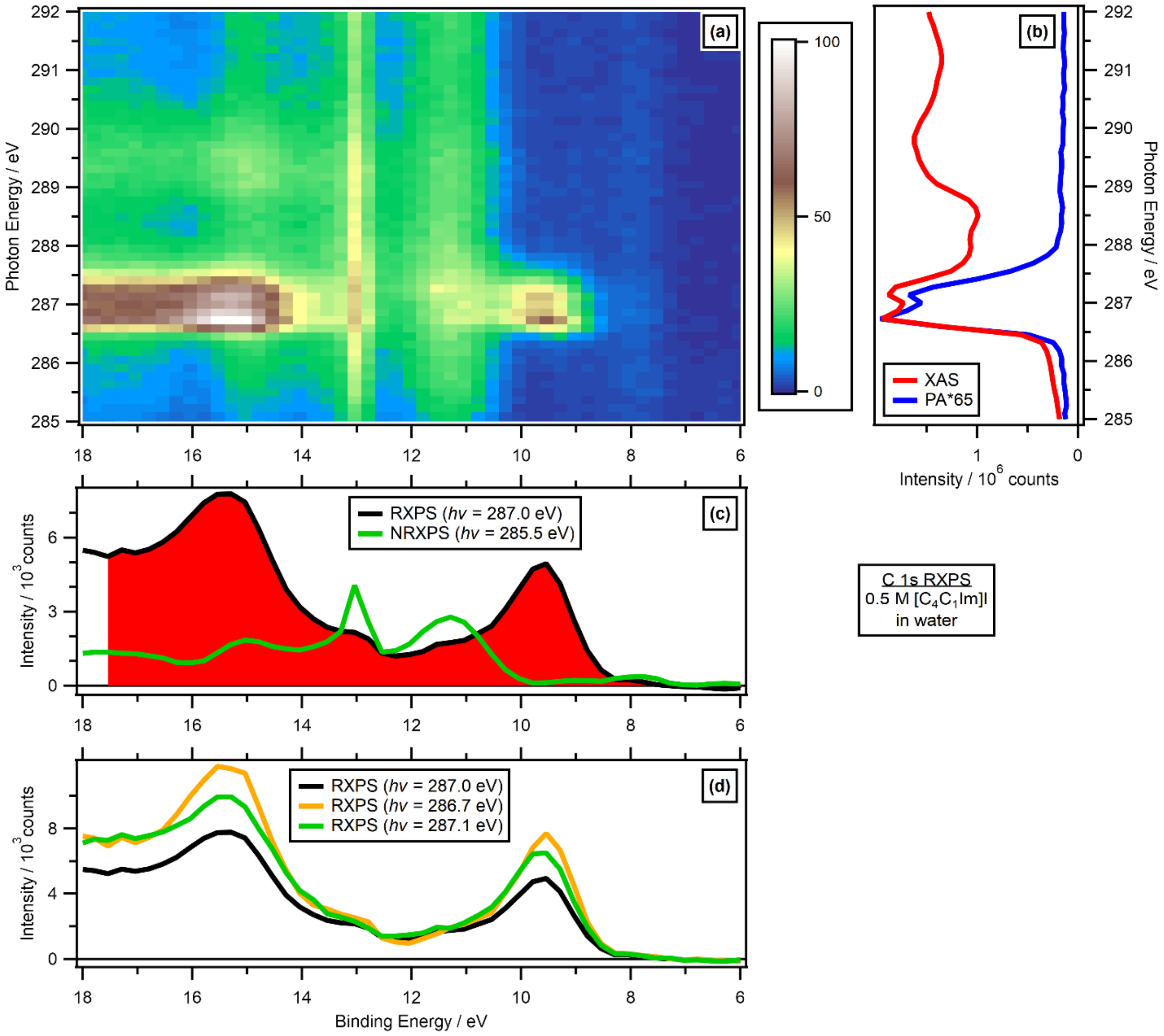

Figure S14. C 1s RXPS for 0.5 M [C_4C_1Im]I in water. (a) C 1s valence RXPS heat map for 0.5 M [C_4C_1Im]I in water. (b) Partial electron yield C 1s NEXAFS spectra (spectator Auger region plus participator Auger region = XAS, and participator Auger region only). (c) C 1s valence NRXP spectrum ($h\nu$ = 285.5 eV) and C 1s valence RXP spectrum ($h\nu$ = 287.0 eV, with the valence NRXPS contributions subtracted; estimated participator Auger contribution shaded red). The NRXPS contributions were subtracted using the procedure outlined in reference [2]. (d) C 1s valence NRXP spectra with the valence NRXPS contributions subtracted ($h\nu$ = 287.0 eV, $h\nu$ = 286.7 eV and $h\nu$ = 287.1 eV). All electron spectra were charge referenced using procedures outlined in Section 2.5.

5.5. RXPS maps: 0.5 M $[C_4C_1Im][N(CN)_2]$ in water

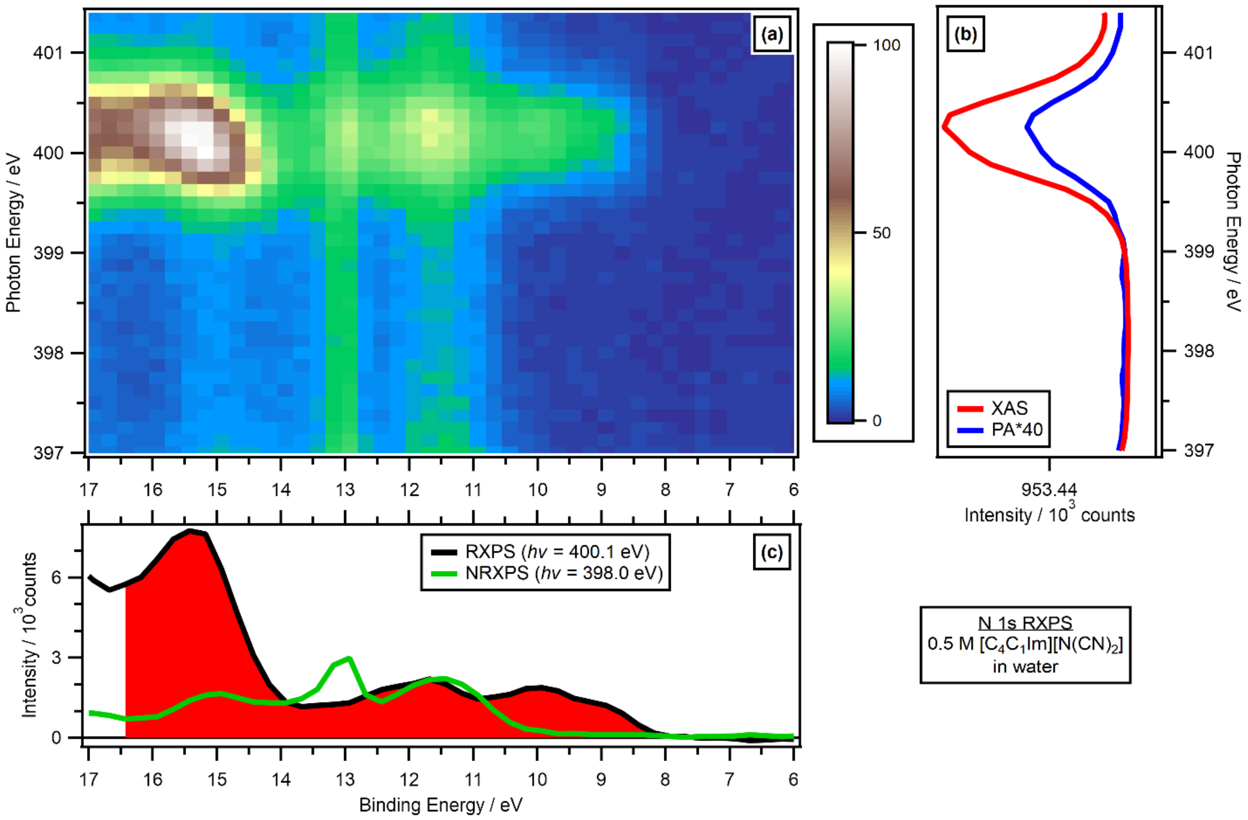

Figure S15. N 1s RXPS for 0.5 M $[C_4C_1Im][N(CN)_2]$ in water. (a) N 1s valence RXPS heat map for 0.5 M $[C_4C_1Im][N(CN)_2]$ in water. (b) Partial electron yield N 1s NEXAFS spectra (spectator Auger region plus participator Auger region = XAS, and participator Auger region only). (c) N 1s valence NRXP spectrum ($h\nu$ = 398.0 eV) and N 1s valence RXP spectrum ($h\nu$ = 400.1 eV, with the valence NRXPS contributions subtracted; estimated participator Auger contribution shaded red). The NRXPS contributions were subtracted using the procedure outlined in reference [2]. All electron spectra were charge referenced using procedures outlined in Section 2.5.

5.6. RXPS maps: 0.5 M $[C_4C_1Im][SCN]$ in water

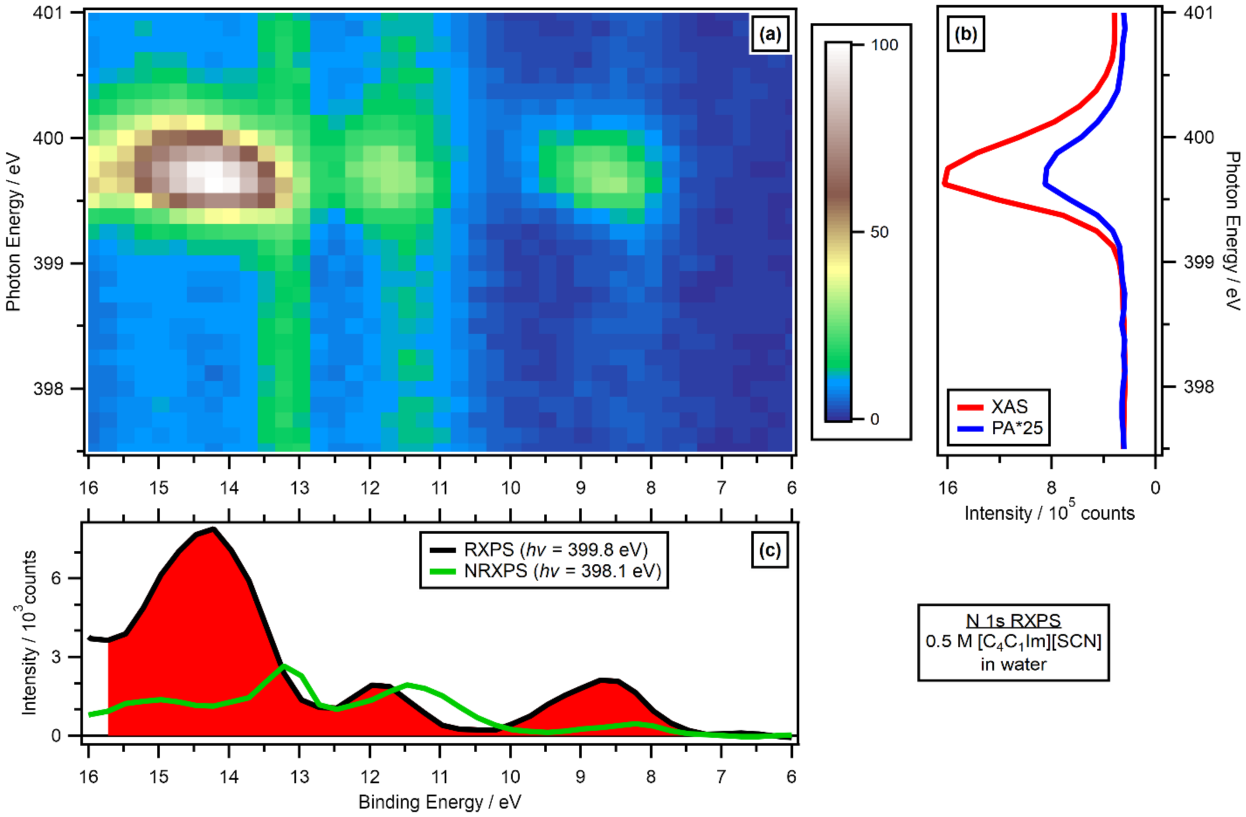

Figure S16. N 1s RXPS for 0.5 M $[C_4C_1Im][SCN]$ in water. (a) N 1s valence RXPS heat map for 0.5 M $[C_4C_1Im][SCN]$ in water. (b) Partial electron yield N 1s NEXAFS spectra (spectator Auger region plus participator Auger region = XAS, and participator Auger region only). (c) N 1s valence NRXP spectrum ($h\nu$ = 398.1 eV) and N 1s valence RXP spectrum ($h\nu$ = 399.8 eV, with the valence NRXPS contributions subtracted; estimated participator Auger contribution shaded red). The NRXPS contributions were subtracted using the procedure outlined in reference [2]. All electron spectra were charge referenced using procedures outlined in Section 2.5.

5.7. RXPS maps: 1.3 M $[C_4C_1Im][OAc]$ in water

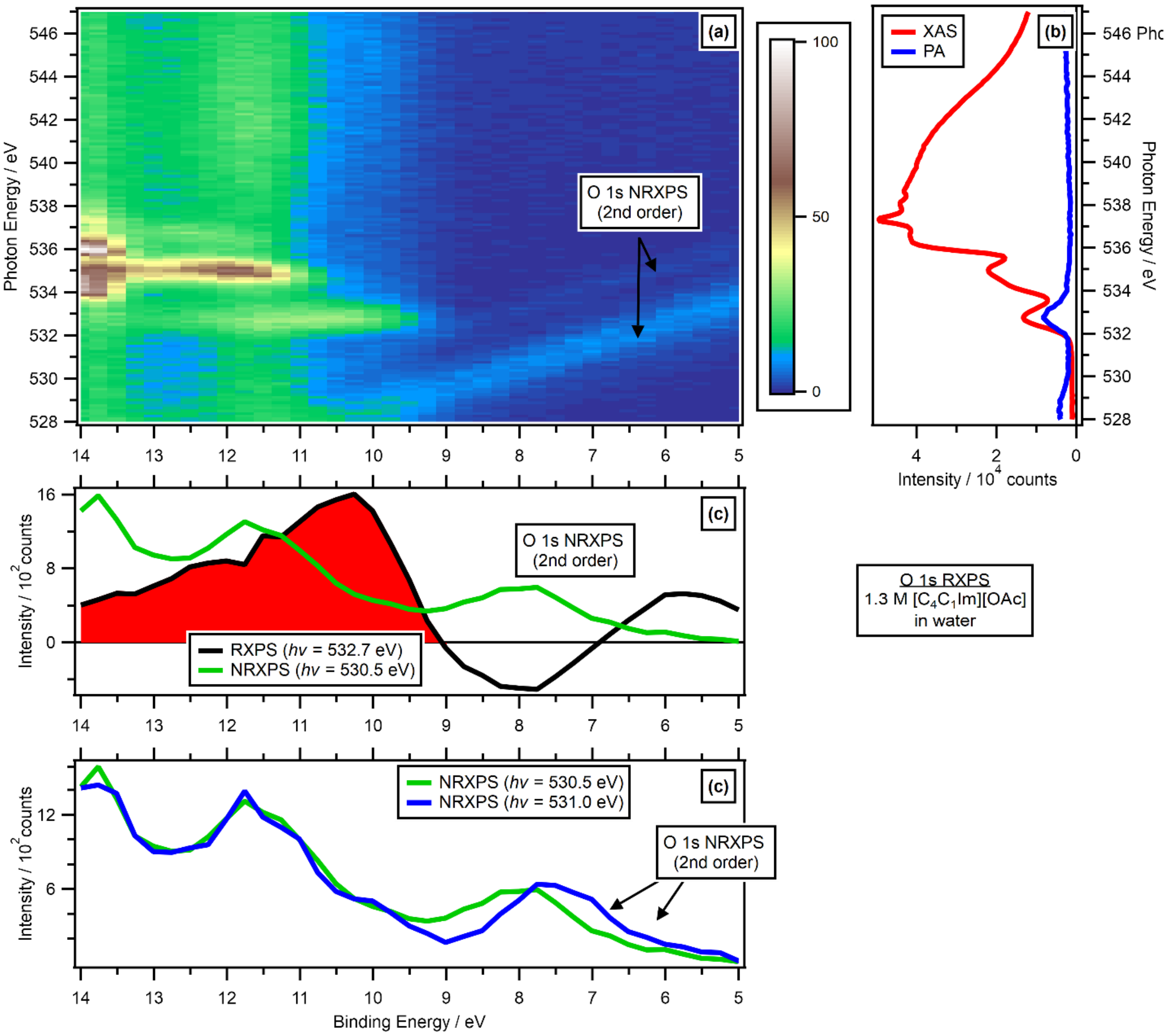

Figure S17. O 1s RXPS for 1.3 M $[C_4C_1Im][OAc]$ in water. (a) O 1s valence RXPS heat map for 1.3 M $[C_4C_1Im][OAc]$ in water. (b) Partial electron yield O 1s NEXAFS spectra (spectator Auger region plus participator Auger region = XAS, and participator Auger region only). (c) O 1s valence NRXP spectrum ($h\nu$ = 530.5 eV) and O 1s valence RXP spectrum ($h\nu$ = 532.7 eV, with the valence NRXPS contributions subtracted; estimated participator Auger contribution shaded red). (d) O 1s valence NRXP spectra ($h\nu$ = 530.5 eV and $h\nu$ = 531.0 eV) depicting the overlap of peaks due to 2nd order light with RXPS contributions. The NRXPS contributions were subtracted using the procedure outlined in reference [2]. All electron spectra were charge referenced using procedures outlined in Section 2.5.

5.8. RXPS maps: 0.5 M [C_4C_1Im][OAc] in MeCN

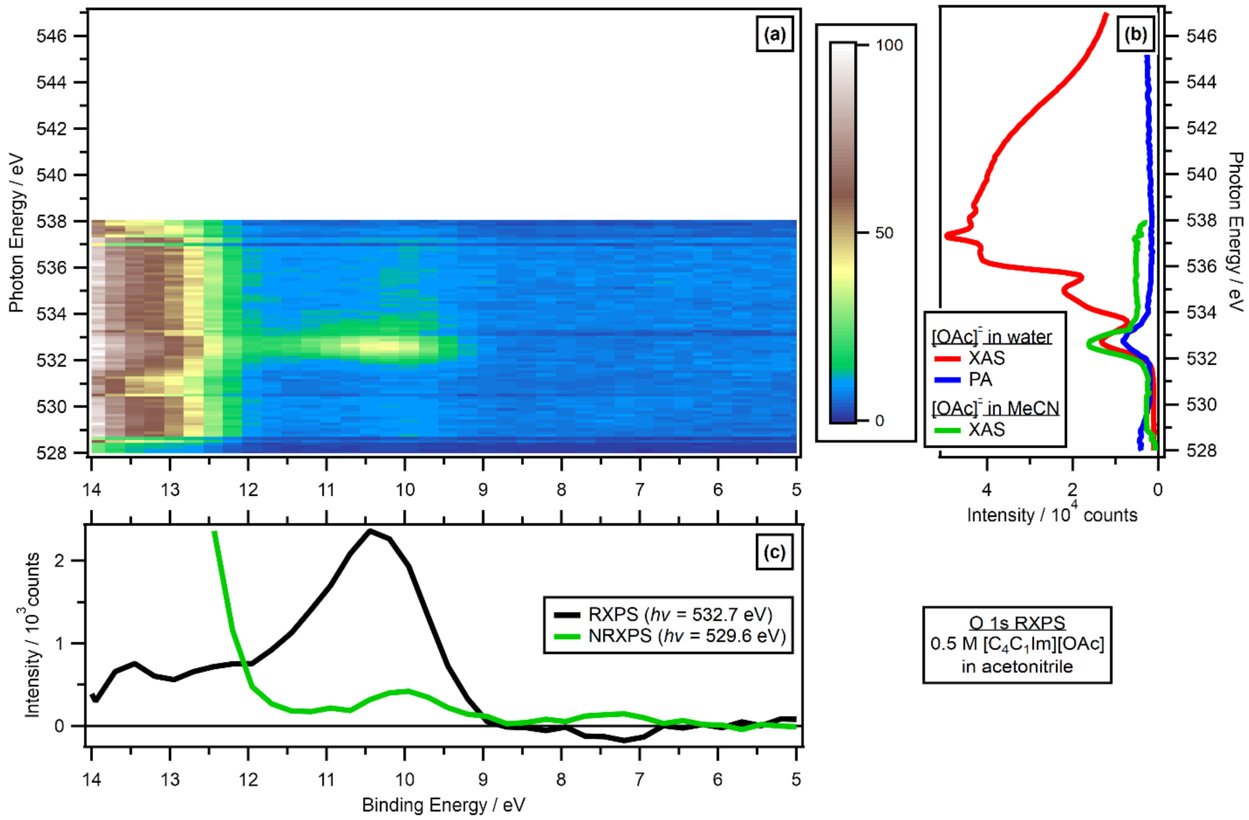

Figure S18. O 1s RXPS for 0.5 M [C_4C_1Im][OAc] in MeCN. (a) O 1s valence RXPS heat map for 0.5 M [C_4C_1Im][OAc] in MeCN. (b) Partial electron yield O 1s NEXAFS spectra (spectator Auger region plus participator Auger region = XAS, and data from Figure S16b). (c) O 1s valence NRXP spectrum ($h\nu$ = 529.6 eV) and O 1s valence RXP spectrum ($h\nu$ = 532.7 eV, with the valence NRXPS contributions subtracted; estimated participator Auger contribution shaded red). The NRXPS contributions were subtracted using the procedure outlined in reference [2]. All electron spectra were charge referenced using procedures outlined in Section 2.5.

5.9. RXPS maps: 0.5 M [C_4C_1Im][TfO] in water

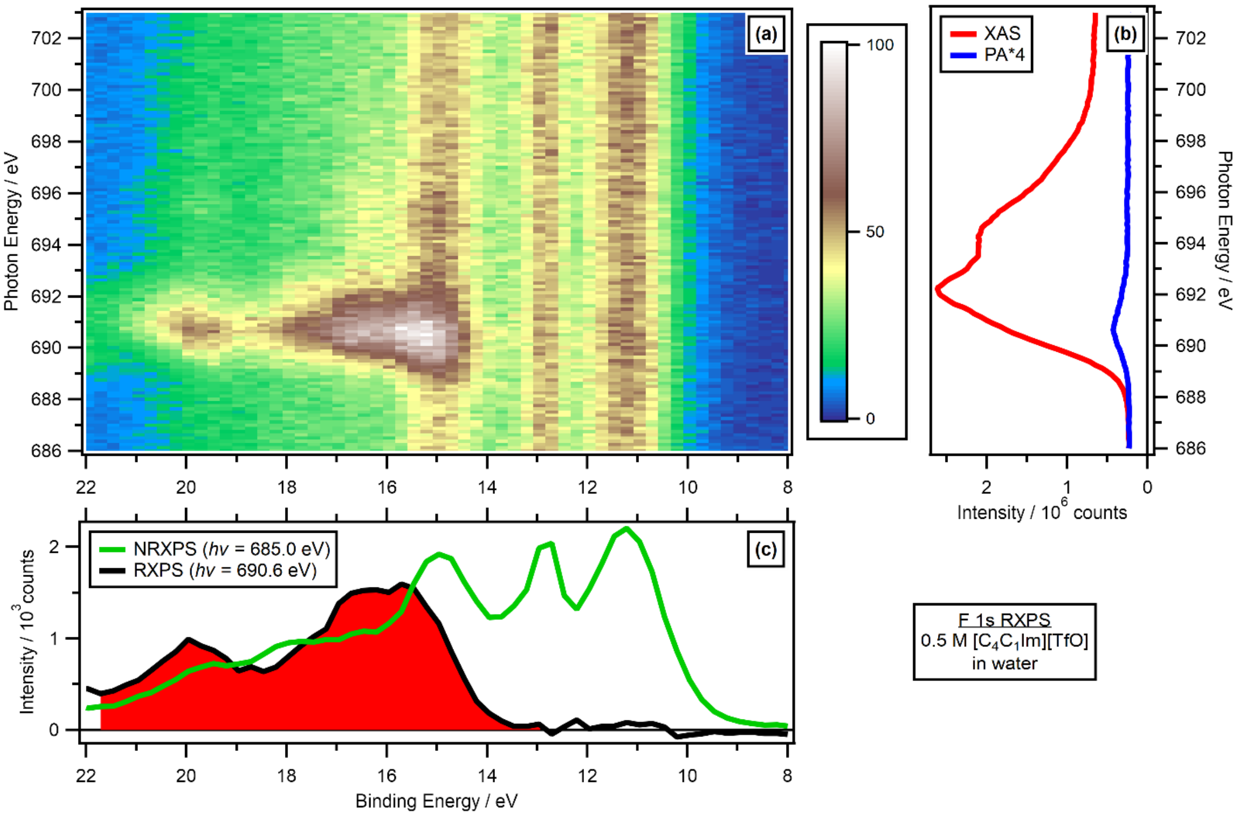

Figure S19. F 1s RXPS for 0.5 M [C_4C_1Im][TfO] in water. (a) F 1s valence RXPS heat map for 0.5 M [C_4C_1Im][TfO] in water. (b) Partial electron yield F 1s NEXAFS spectra (spectator Auger region plus participator Auger region = XAS, and participator Auger region only). (c) F 1s valence NRXP spectrum ($h\nu$ = 685.0 eV) and F 1s valence RXP spectrum ($h\nu$ = 690.6 eV, with the valence NRXPS contributions subtracted; estimated participator Auger contribution shaded red). The NRXPS contributions were subtracted using the procedure outlined in reference [2]. All electron spectra were charge referenced using procedures outlined in Section 2.5.

5.10. RXPS maps: 1.0 M [$N_{4,1,1,0}$][HSO_4] in water

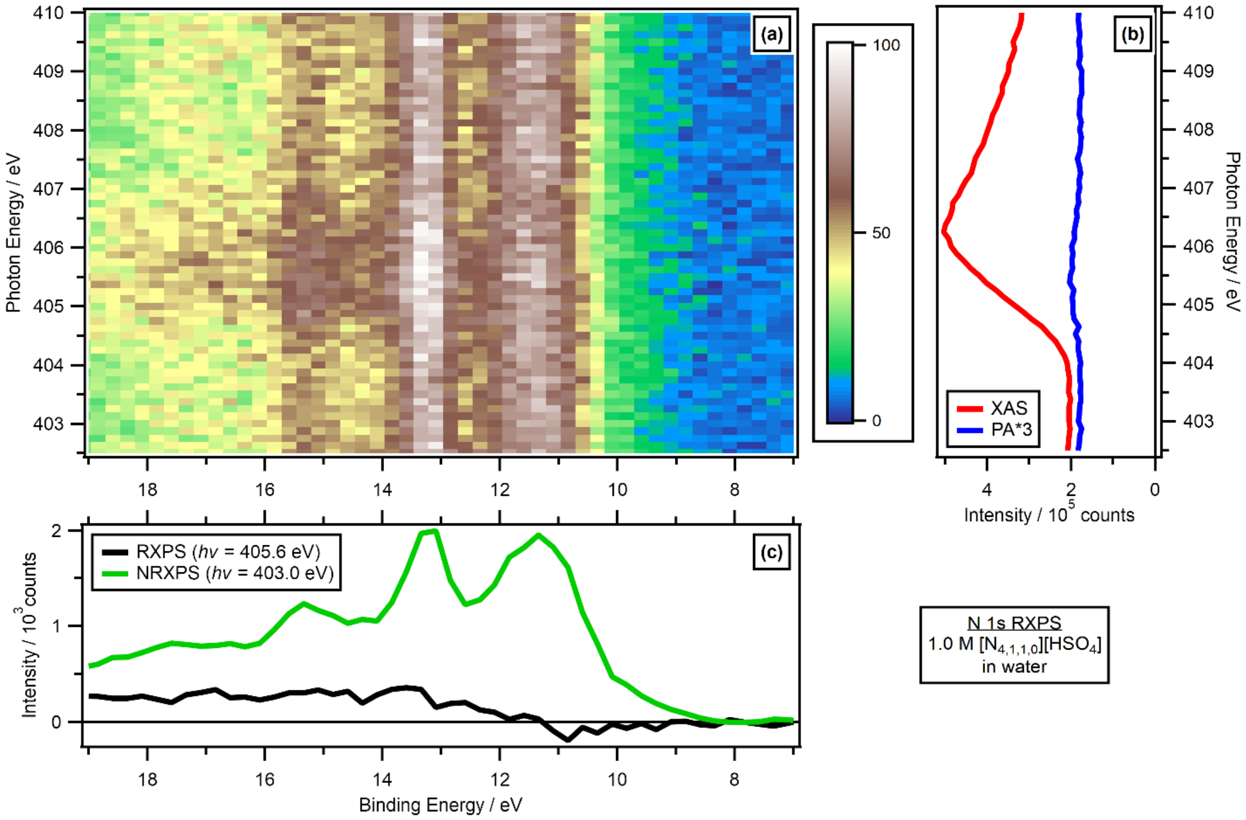

Figure S20. N 1s RXPS for 1.0 M [$N_{4,1,1,0}$][HSO_4] in water. (a) N 1s valence RXPS heat map for 1.0 M [$N_{4,1,1,0}$][HSO_4] in water. (b) Partial electron yield N 1s NEXAFS spectra (spectator Auger region plus participator Auger region = XAS, and participator Auger region only). (c) N 1s valence NRXP spectrum ($h\nu$ = 403.0 eV) and N 1s valence RXP spectrum ($h\nu$ = 405.6 eV, with the valence NRXPS contributions subtracted; estimated participator Auger contribution shaded red). The NRXPS contributions were subtracted using the procedure outlined in reference [2]. All electron spectra were charge referenced using procedures outlined in Section 2.5.

5.11. RXPS maps: 3.3 M $[N_{4,1,1,0}][HSO_4]$ in water

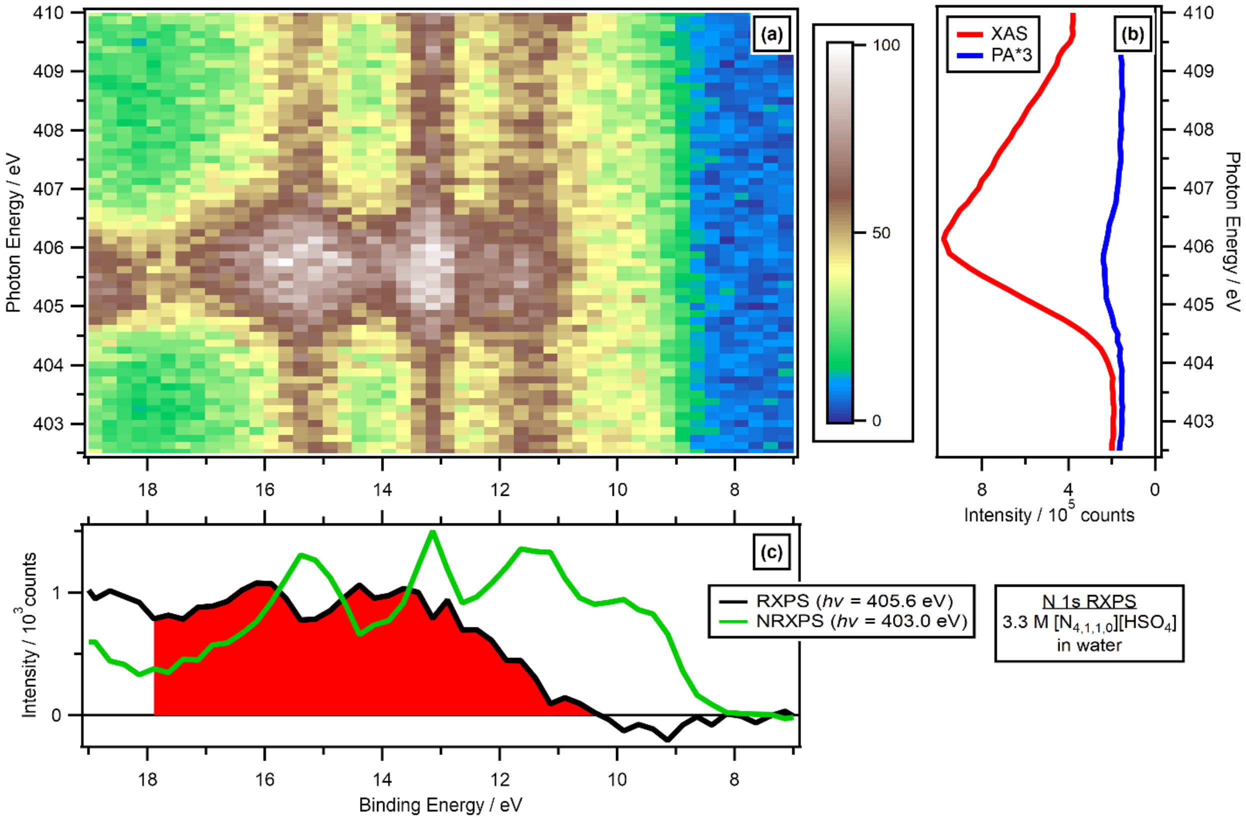

Figure S21. N 1s RXPS for 3.3 M $[N_{4,1,1,0}][HSO_4]$ in water. (a) N 1s valence RXPS heat map for 3.3 M $[N_{4,1,1,0}][HSO_4]$ in water. (b) Partial electron yield N 1s NEXAFS spectra (spectator Auger region plus participator Auger region = XAS, and participator Auger region only). (c) N 1s valence NRXP spectrum ($h\nu$ = 403.0 eV) and N 1s valence RXP spectrum ($h\nu$ = 405.6 eV, with the valence NRXPS contributions subtracted; estimated participator Auger contribution shaded red). The NRXPS contributions were subtracted using the procedure outlined in reference [2]. All electron spectra were charge referenced using procedures outlined in Section 2.5.

6. Laboratory XPS

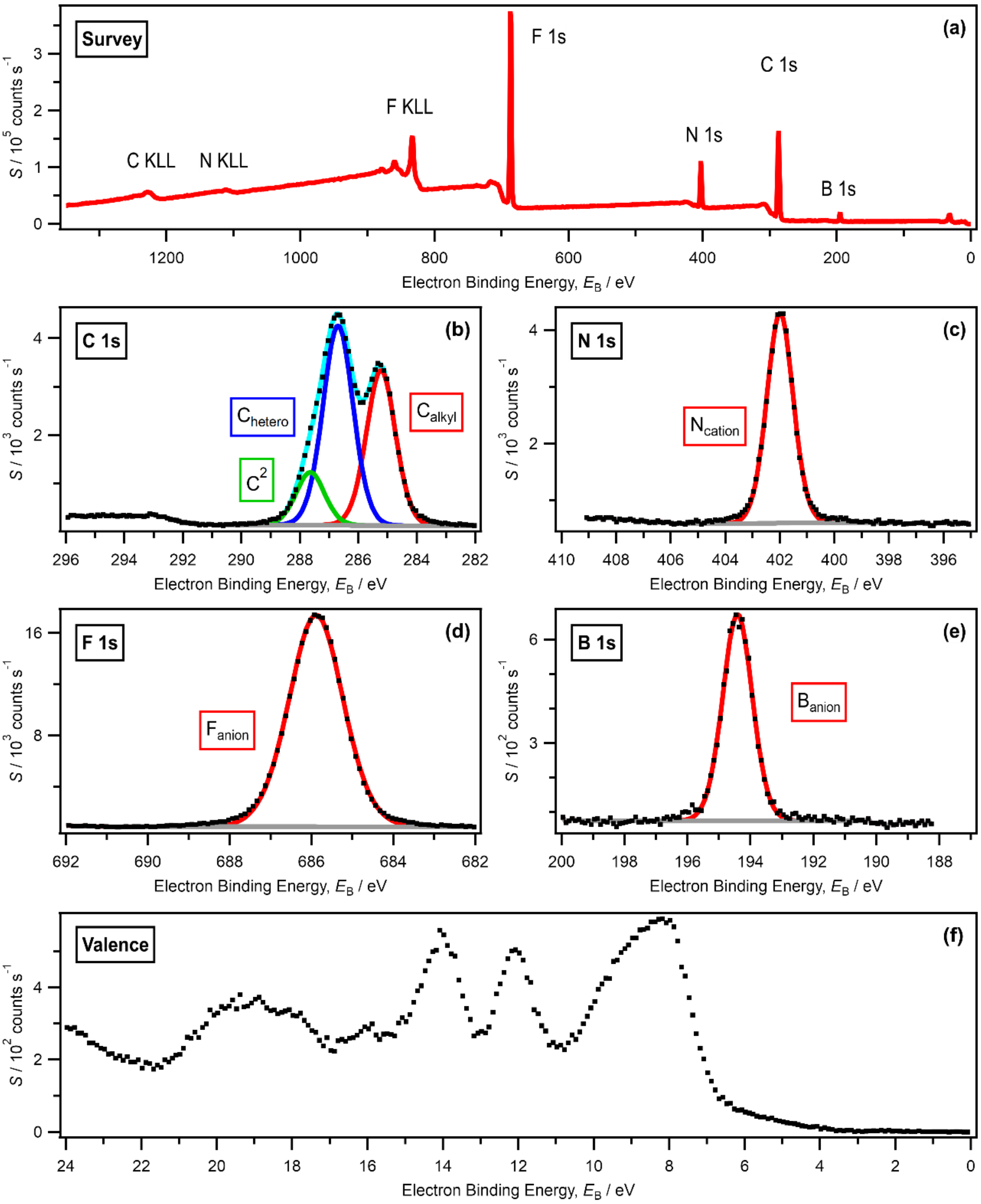

Figure S22. (a) Survey, (b-e) core and (f) valence XP spectra for $[C_4C_1Im][BF_4]$ recorded on laboratory–based XPS apparatus at $h\nu = 1486.6$ eV. All XP spectra were charge referenced to $E_B(C_{alkyl}\ 1s) = 285.00$ eV, to match that used for previous publications on neat ionic liquids (e.g. reference [1, 2]).

7. Factors determining RXPS intensity

ESI Table S4. RXPS:NRXPS intensity ratios.

Sample	Edge	Upper E_B / eV	Lower E_B / eV	RXPS:NRXPS intensity ratio
$[TfO]^-$	F 1s	20.5	12.7	2
EtOH	O 1s	10.5	8.7	1
Water	O 1s	12.1	10.5	1
PC	O 1s	11.4	10.0	2
$[SCN]^-$	N 1s	8.9	6.9	4
$[N(CN)_2]^-$	N 1s	9.9	8.1	3
$[C_8C_1Im]^+$	N 1s	11.3	9.3	3
$[TfO]^-$	O 1s	13.0	9.0	4
PC	O 1s	11.4	10.0	6
$[CoCl_4]^{2-}$	Co $2p_{3/2}$	9.7	7.8	4
$[CoCl_4]^{2-}$	Co $2p_{3/2}$	11.7	9.8	6
$[CoCl_4]^{2-}$	Co $2p_{3/2}$	14.8	12.9	9
$[C(CN)_3]^-$	N 1s	8.6	6.6	20
$[C(CN)_3]^-$	N 1s	8.6	6.6	21
$[C_4C_1Im]^+$	C 1s	9.7	8.9	16
$[C_4C_1Im]^+$	C 1s	9.7	8.9	14
MeCN	N 1s	12.1	10.7	94
MeCN	N 1s	13.7	12.3	133

8. Further RXPS explanations

$[C_4C_1Im]^+$

The $[C_4C_1Im]^+$ C 1s NEXAFS spectrum showed two C 1s → π* absorptions at $h\nu$ = 286.7 eV and $h\nu$ = 287.1 eV (Figure S14b), matching to literature values.[18] Based on C 1s NRXPS and calculations,[18, 19] the absorption at $h\nu$ = 286.7 eV was due to the two N-C-C-N C_{ring} atoms and the absorption at $h\nu$ = 287.1 eV was due to the N-C-N C_{ring} atom. The C 1s RXPS traces for these two absorptions were essentially identical (Figure S14d), demonstrating that the same occupied valence states contributed to both RXPS traces.

Imidazole

The imidazole N 1s NEXAFS spectrum showed two N 1s → π* absorptions at $h\nu$ = 400.2 eV and $h\nu$ = 401.9 eV (ESI Figure S9b), matching to literature values.[20] Based on N 1s NRXPS,[21] the absorption at $h\nu$ = 400.2 eV was due to the C-N=C atom and the absorption at $h\nu$ = 401.9 eV was due to C-NH-C atom. The N 1s RXPS traces for these two absorptions were essentially identical (ESI Figure S9c and ESI Figure S9d), demonstrating that the same occupied valence states contributed to both RXPS traces, especially the feature at lowest E_B.

PC

The PC C 1s RXPS trace at the C 1s → π* absorption at $h\nu$ = 290.5 eV matched well in terms of E_B to the O 1s NRXPS trace for C=O (Figure 7a). We were unable to find literature calculations of the C 1s NEXAFS spectrum for PC, but the excellent visual match suggests that this C 1s RXPS trace represents the OVSs for the carbon contributions to C=O.

$[C(CN)_3]^-$

$[C(CN)_3]^-$ gave one symmetric peak in N 1s NRXPS,[2, 22] and two π* absorptions in the N 1s NEXAFS spectrum ($h\nu$ = 399.0 eV and $h\nu$ = 400.0 eV, reference [2, 22, 23]). Therefore, the three nitrogen atoms in $[C(CN)_3]^-$ are on average in the same electronic state.

$[BF_4]^-$

The $[BF_4]^-$ B 1s RXPS gave very weak signals. Therefore, subtraction of the very intense solvent water valence NRXPS contributions to produce the B 1s RXPS data meant experimental PA contributions for $[BF_4]^-$ B 1s RXPS at 16 eV > E_B > 10 eV could not be ruled out, based on the experimental data. However, there were no boron contributions to the DoS at 16 eV > E_B > 10 eV (Figure 4d and Figure 7e), demonstrating that the B 1s RXPS were accurate, in spite of the challenges of removing the valence NRXPS contributions of the solvent.

9. Valence RXPS traces versus pDoS calculations

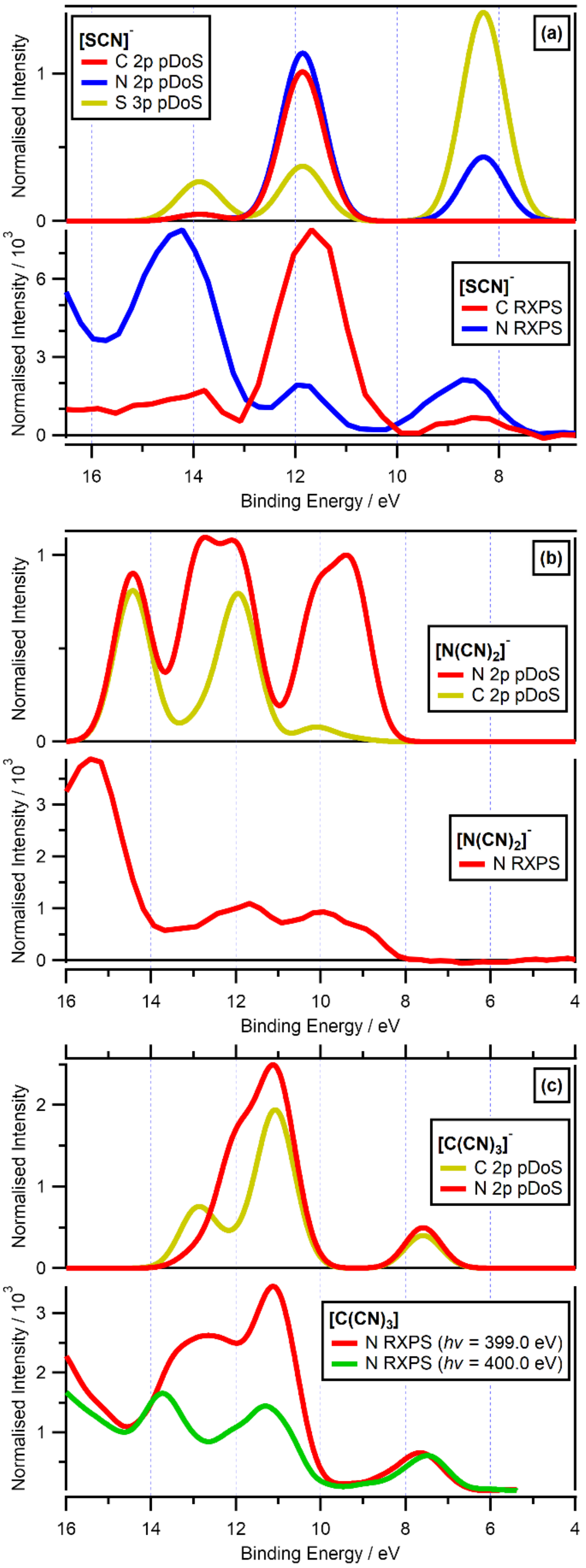

Figure S23. Participator Auger regions for valence RXP spectra at different absorption edges with the valence NRXPS contributions subtracted, compared to lone ion SMD pDoS calculations. (a) N 1s valence NRXP spectrum for 0.5 M $[C_4C_1Im][SCN]$ in water ($h\nu$ = 399.8 eV) and C 1s valence NRXP spectrum for 0.5 M K[SCN] in water ($h\nu$ = 287.5 eV), compared to C 2p, N 2p and S 3p pDoS calculated for lone $[SCN]^-$ in an SMD. (b) N 1s valence NRXP spectrum for 0.5 M $[C_4C_1Im][N(CN)_2]$ in water ($h\nu$ = 400.1 eV), compared to N 2p pDoS calculated for lone $[N(CN)_2]^-$ in an SMD. (c) N 1s valence NRXP spectrum for $[C_8C_1Im][C(CN)_3]$ ($h\nu$ = 399.0 eV and $h\nu$ = 400.0 eV), compared to C 2p and N 2p pDoS calculated for lone $[C(CN)_3]^-$ in an SMD. The NRXPS contributions were subtracted using the procedure outlined in reference [2]. All electron spectra were charge referenced using procedures outlined in Section 2.5.

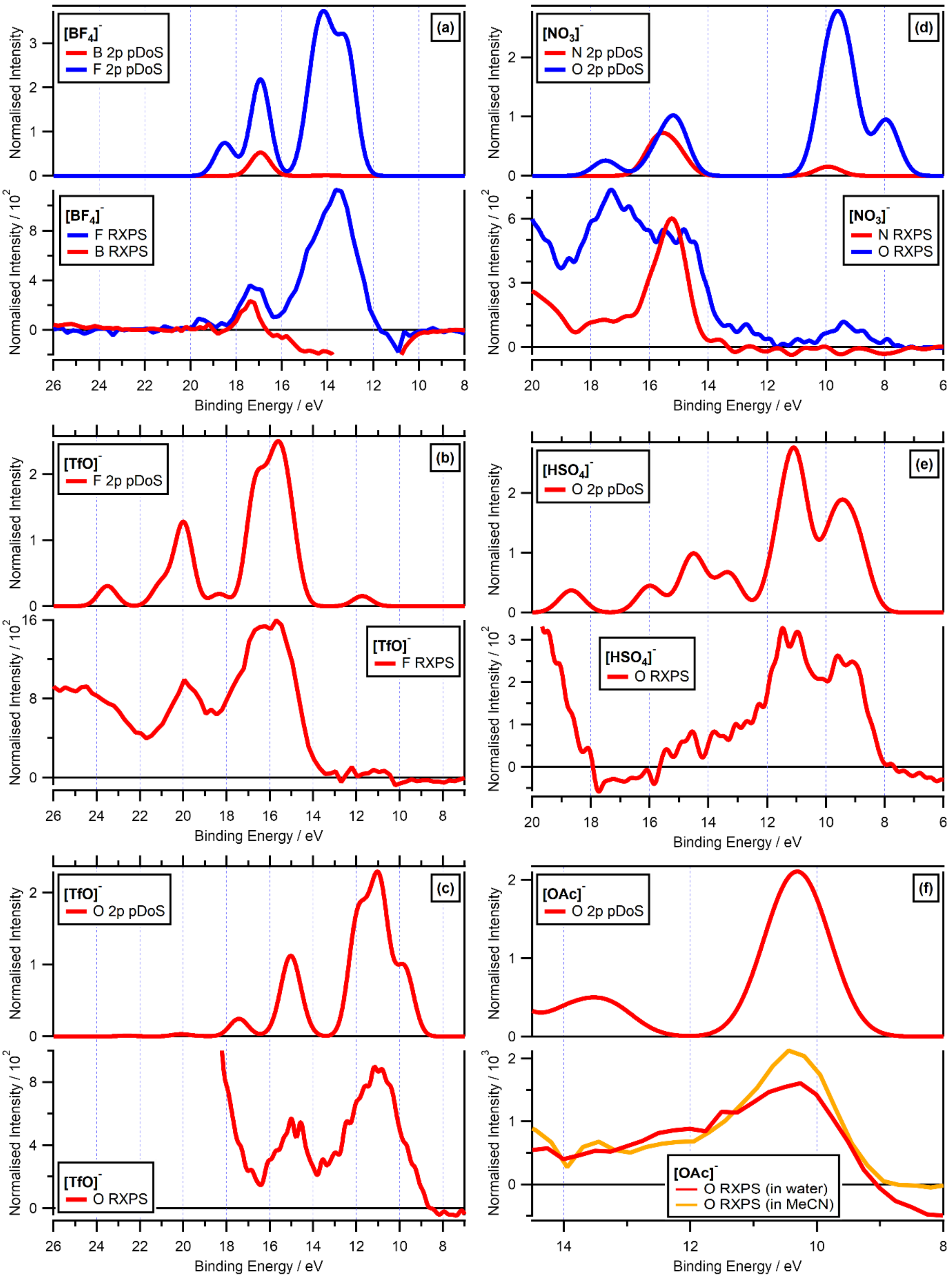

Figure S24. Participator Auger regions for valence RXP spectra at different absorption edges with the valence NRXPS contributions subtracted, compared to lone ion SMD pDoS calculations. (a) B 1s and F 1s edge data for 0.5 M $[C_4C_1Im][BF_4]$ in water ($h\nu = 201.4$ eV and $h\nu = 696.4$ eV, respectively), compared to B 2p and F 2p pDoS calculated for lone $[BF_4]^-$ in an SMD. (b) F 1s edge data for 0.5 M $[C_4C_1Im][TfO]$ in water ($h\nu = 690.6$ eV), compared to F 2p pDoS calculated for lone $[TfO]^-$ in an SMD. (c) O 1s edge data for $[N_{2,2,1,0}][TfO]$ ($h\nu = 535.3$

eV), compared to O 2p pDoS calculated for lone [TfO]$^-$ in an SMD. (d) N 1s and O 1s edge data for [$P_{6,6,6,14}$][NO_3] ($h\nu$ = 405.0 eV and $h\nu$ = 529.0 eV, respectively), compared to N 2p and O 2p pDoS calculated for lone [NO_3]$^-$ in an SMD. (e) O 1s edge data for [$N_{4,1,1,0}$][HSO_4] ($h\nu$ = 531.0 eV), compared to O 2p pDoS calculated for lone [HSO_4]$^-$ in an SMD. (f) O 1s edge data for [C_4C_1Im][OAc] ($h\nu$ = 532.7 eV) in both water and MeCN, compared to O 2p pDoS calculated for lone [OAc]$^-$ in an SMD. The NRXPS contributions were subtracted using the procedure outlined in reference [2]. All electron spectra were charge referenced using procedures outlined in Section 2.5.

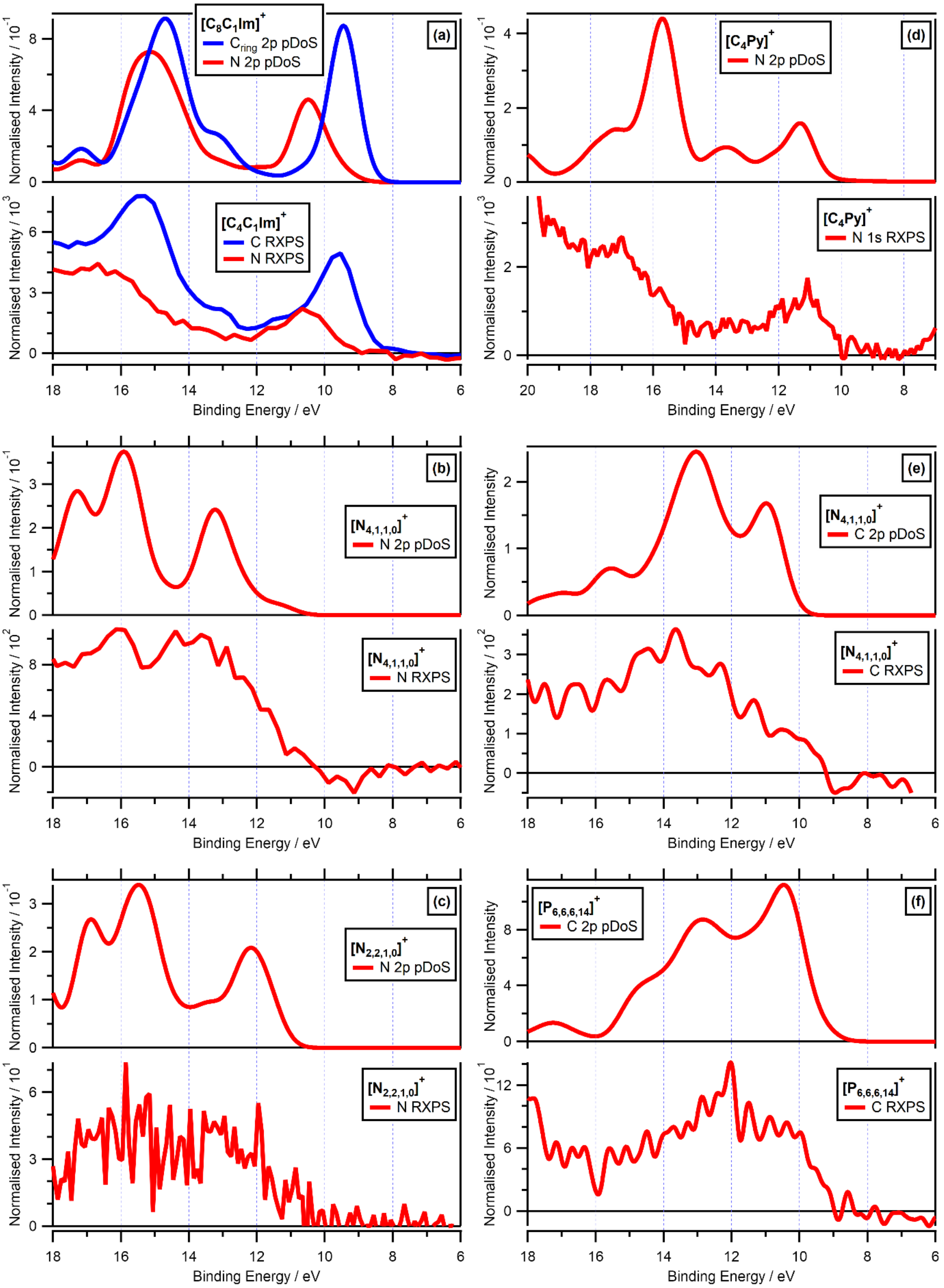

Figure S25 Participator Auger regions for valence RXP spectra at different absorption edges with the valence NRXPS contributions subtracted, compared to lone ion SMD pDoS calculations. (a) C 1s and N 1s valence RXP spectra for 0.5 M [C$_4$C$_1$Im]I in water ($h\nu$ = 287.0 eV and $h\nu$ = 402.1 eV, respectively), compared to C$_{ring}$ 2p and N 2p pDoS calculated for lone [C$_4$C$_1$Im]$^+$ in an SMD. (b) N 1s valence RXP spectrum for 3.3 M [N$_{4,1,1,0}$][HSO$_4$] in water ($h\nu$ = 405.6 eV), compared to N 2p pDoS calculated for lone [N$_{4,1,1,0}$]$^+$ in an SMD. (c) N 1s valence RXP spectrum for 0.5 M $[N_{2,2,1,0}]$[TfO] in water ($h\nu$ = 405.0 eV), compared to N 2p pDoS calculated for lone $[N_{2,2,1,0}]^+$ in an SMD. (d) N 1s valence RXP spectrum for $[C_4Py][NTf_2]$ ($h\nu$ = 401.0 eV), compared to N 2p pDoS calculated for lone $[C_4Py]^+$ in an SMD. (e) C 1s valence RXP spectrum for $[N_{4,1,1,0}][HSO_4]$ ($h\nu$ = 288.0 eV), compared to N 2p pDoS calculated for lone $[N_{4,1,1,0}]^+$ in an SMD. (f) C 1s valence RXP spectrum for $[P_{6,6,6,14}][NO_3]$ ($h\nu$ = 287.0 eV), compared to C 2p pDoS calculated for lone $[P_{6,6,6,14}]^+$ in an SMD. The NRXPS contributions were subtracted using the procedure outlined in reference [2]. All electron spectra were charge referenced using procedures outlined in Section 2.5.

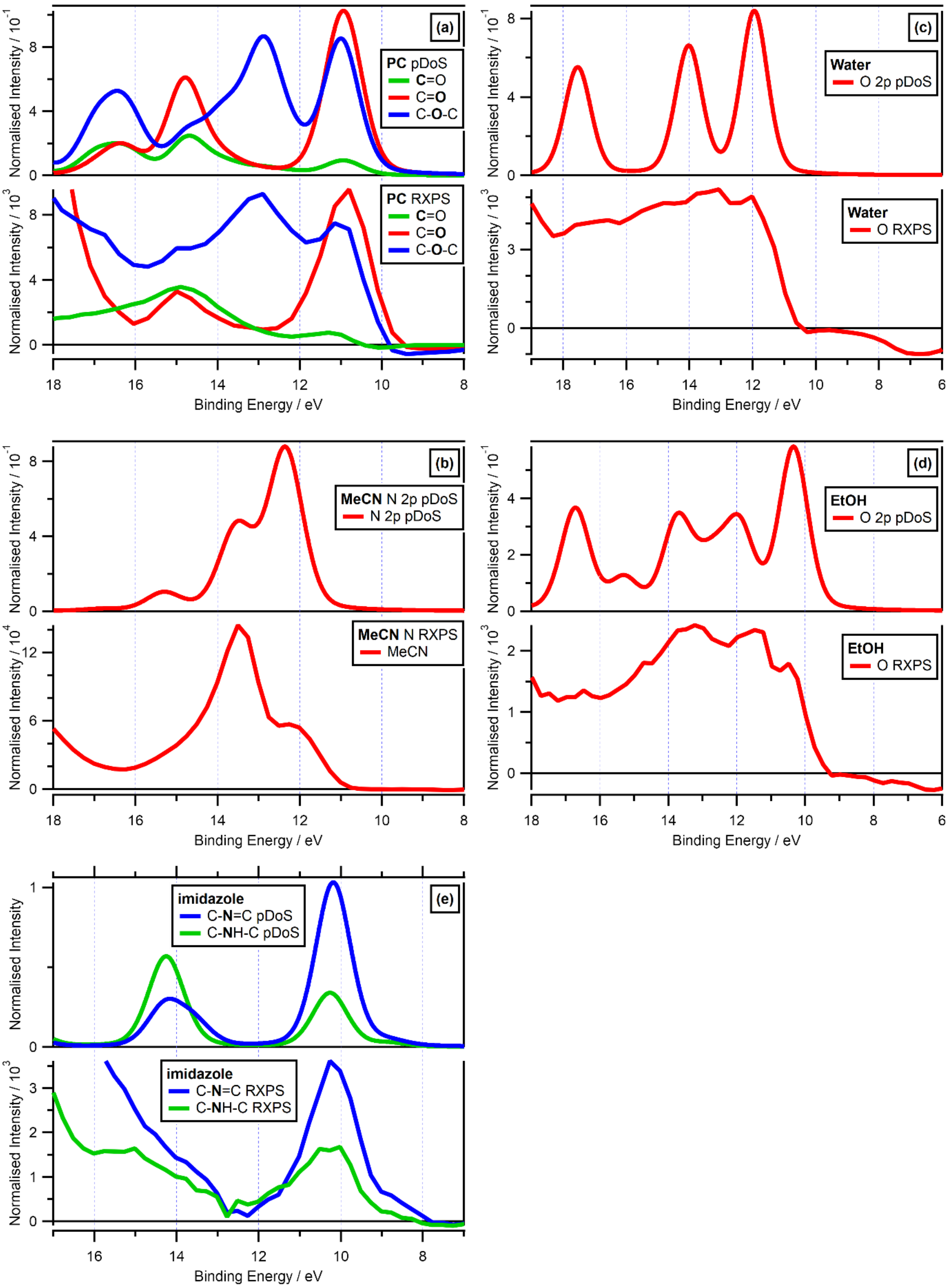

Figure S26 Participator Auger regions for valence RXP spectra at different absorption edges with the valence NRXPS contributions subtracted, compared to lone ion SMD pDoS calculations. (a) O 1s valence RXP spectra for propylene carbonate (PC) at both the C=O and C-O-C absorption edges ($h\nu$ = 533.3 eV and $h\nu$ = 536.2 eV respectively), and C 1s valence RXP spectrum for propylene carbonate (PC) at the C=O absorption edge ($h\nu$ = 290.5 eV), compared to C=O O pDoS, C-O-C O pDoS and C=O C pDoS calculated for PC in an SMD. (b) N 1s valence RXP spectrum for MeCN ($h\nu$ = 400.1 eV), compared to N 2p pDoS calculated for lone MeCN in an SMD. (c) O 1s valence RXP spectrum for water ($h\nu$ = 535.0 eV), compared to O 2p pDoS calculated for lone water in an SMD. (d) O 1s valence RXP spectrum for EtOH ($h\nu$ = 535.4 eV), compared to N 2p pDoS calculated for lone EtOH in an SMD. (e) N 1s valence RXP spectra for 1.8 M imidazole in water at both the C-N=C and C-NH-C absorption edges ($h\nu$ = 400.2 eV and $h\nu$ = 401.9 eV respectively), compared to C-N=C and C-NH-C N pDoS calculated for imidazole in an SMD. The NRXPS contributions were subtracted using the procedure outlined in reference [2]. All electron spectra were charge referenced using procedures outlined in Section 2.5.

10. Structures from DFT

10.1. $[SCN]^-$

Table S5. $[SCN]^-$ (SMD). Units in Ångströms. Cartesian axes.

Atom	X	Y	Z
C	0.00000	0.00000	-0.63032
N	0.00000	0.00000	-1.80650
S	0.00000	0.00000	1.02671

10.2. $[N(CN)_2]^-$

Table S6. $[N(CN)_2]^-$ (SMD). Units in Ångströms. Cartesian axes.

Atom	X	Y	Z
C	0.01262	0.50658	-0.01158
N	0.43348	-0.37164	-0.66170
C	-1.39190	1.58605	1.45043
N	-2.29813	1.72750	2.17832
N	-0.35625	1.55424	0.66473

10.3. $[C(CN)_3]^-$

Table S7. $[C(CN)_3]^-$ (SMD). Units in Ångströms. Cartesian axes.

Atom	X	Y	Z
C	-1.20092	0.75904	0.67190
C	-2.60402	0.75904	0.67190
C	-0.49910	-0.45589	0.67190
C	-0.49910	1.97397	0.67190
N	0.08208	2.98174	0.67190
N	0.08208	-1.46366	0.67190
N	-3.76737	0.75904	0.67190

10.4. $[BF_4]^-$

Table S8. $[BF_4]^-$ (SMD). Units in Ångströms. Cartesian axes.

Atom	X	Y	Z
B	-1.42561	0.96494	0.00000
F	-0.95406	1.63125	1.15377
F	-2.83895	0.96462	0.00000
F	-0.95406	1.63124	-1.15377
F	-0.95451	-0.36748	0.00000

10.5. $[TfO]^-$

Table S9. $[TfO]^-$ (SMD). Units in Ångströms. Cartesian axes.

Atom	X	Y	Z
S	0.00000	-0.00063	0.91659
O	0.00001	1.43840	1.24843
O	1.24595	-0.71923	1.25161
O	-1.24596	-0.71921	1.25161
C	0.00000	-0.00032	-0.96415
F	-0.00001	-1.25447	-1.44715
F	-1.08641	0.62774	-1.44494
F	1.08641	0.62773	-1.44494

10.6. $[NO_3]^-$

Table S10. $[NO_3]^-$ (SMD). Units in Ångströms. Cartesian axes.

Atom	X	Y	Z
N	0.50484	0.54173	0.00000
O	0.50669	1.17007	-1.08864
O	0.50666	-0.71547	0.00000
O	0.50115	1.17006	1.08864

10.7. $[HSO_4]^-$

Table S11. $[HSO_4]^-$ (SMD). Units in Ångströms. Cartesian axes.

Atom	X	Y	Z
S	0.14019	-0.02847	0.00001
O	0.31557	-0.82086	1.23743
O	0.82345	1.27714	0.00006
O	0.31559	-0.82077	-1.23747
O	-1.46549	0.44061	0.00000
H	-2.02428	-0.35253	-0.00005

10.8. $[OAc]^-$

Table S12. $[OAc]^-$ (SMD). Units in Ångströms. Cartesian axes.

Atom	X	Y	Z
C	1.16916	0.21932	0.00051
O	1.77564	1.32607	-0.01337
O	1.71256	-0.92077	0.01288
C	-0.36578	0.23837	0.00058
H	-0.73790	-0.28850	-0.88333
H	-0.73952	-0.29946	0.87704
H	-0.76528	1.25351	0.00598

10.9. $[C_8C_1Im]^+$

Table S13. $[C_8C_1Im]^+$ (SMD). Units in Ångströms. Cartesian axes.

Atom	X	Y	Z
C	-1.02229	1.39854	0.08751
C	-2.29622	1.16113	-0.32736
C	-1.43226	-0.75642	0.35023
N	-0.50250	0.18894	0.50912
H	-0.44726	2.30751	0.12330
H	-3.04903	1.82304	-0.71950
H	-1.31587	-1.79937	0.59134
N	-2.53109	-0.19050	-0.15578
C	0.87541	-0.03411	0.97828
H	1.10287	0.75655	1.69415
H	0.88026	-0.98582	1.50935
C	1.87315	-0.03882	-0.17576
H	1.80410	0.91145	-0.71504
H	1.59918	-0.83074	-0.88063
C	3.30402	-0.25039	0.32059
H	3.36559	-1.20447	0.85800
H	3.55517	0.53237	1.04649
C	4.33136	-0.23757	-0.81289
H	4.26298	0.71664	-1.34996
H	4.07884	-1.01978	-1.53947
C	-3.78255	-0.88227	-0.47152
H	-4.58481	-0.47836	0.14493
H	-4.01484	-0.73806	-1.52594
H	-3.65715	-1.94284	-0.26445
C	5.76743	-0.44173	-0.32720
H	6.01245	0.33372	0.40960
H	5.83835	-1.40118	0.20075
C	6.80049	-0.40772	-1.45501
H	6.72598	0.55084	-1.98455
H	6.56005	-1.18503	-2.19167
C	8.23843	-0.60190	-0.96884
H	8.47249	0.16972	-0.22551
H	8.31567	-1.56380	-0.44766
C	9.26732	-0.54972	-2.09852
H	9.23091	0.41189	-2.62111
H	10.28498	-0.68375	-1.71972
H	9.08202	-1.33533	-2.83851

10.10. $[N_{8,1,1,0}]^+$

Table S14. $[N_{8,1,1,0}]^+$ (SMD). Units in Ångströms. Cartesian axes.

Atom	X	Y	Z
H	-2.80386	0.62415	0.25422
C	-1.46330	1.11487	-1.21574
H	-1.68346	2.17841	-1.14763
H	-0.40289	0.95898	-1.40673
H	-2.06113	0.65213	-1.99828
C	-1.06114	1.11851	1.21492
H	-1.25384	2.18879	1.18183
H	-1.40673	0.70870	2.15953
H	0.00065	0.91951	1.07812
C	-1.58916	-1.02315	0.02451
H	-2.09691	-1.35592	-0.88125
H	-0.51553	-1.16923	-0.10315
C	-2.12535	-1.76069	1.24061
H	-1.58093	-1.46404	2.14045
H	-3.17779	-1.49513	1.39291
C	-1.99918	-3.27596	1.05572
H	-0.94945	-3.53026	0.86673
H	-2.55973	-3.58260	0.16495
C	-2.49985	-4.06133	2.26889
H	-3.55046	-3.80711	2.45634
H	-1.94179	-3.74514	3.15884
C	-2.36714	-5.57596	2.10122
H	-1.31627	-5.82695	1.90934
H	-2.92638	-5.89222	1.21165
C	-2.86044	-6.36607	3.31466
H	-3.91222	-6.11756	3.50615
H	-2.30284	-6.04805	4.20496
N	-1.80441	0.47091	0.09016
C	-2.72376	-7.88148	3.15087
H	-1.67290	-8.12883	2.95804
H	-3.28211	-8.19889	2.26196
C	-3.21708	-8.66243	4.36939
H	-4.27387	-8.45565	4.56826
H	-3.11120	-9.74154	4.22416
H	-2.65219	-8.39032	5.26711

10.11. $[N_{4,1,1,0}]^+$

Table S15. $[N_{4,1,1,0}]^+$ (SMD). Units in Ångströms. Cartesian axes.

Atom	X	Y	Z
N	-0.29004	0.69906	-0.99221
H	-0.86851	0.63886	-1.83466
C	0.83437	1.63370	-1.30190
H	0.41610	2.59431	-1.59593
H	1.44460	1.74405	-0.40725
H	1.42355	1.21311	-2.11408
C	-1.15057	1.23916	0.10261
H	-1.43596	2.25660	-0.15662
H	-2.03843	0.62087	0.20237
H	-0.57533	1.23301	1.02687
C	0.23674	-0.69020	-0.70187
H	0.92985	-0.57519	0.13210
H	0.80098	-0.97949	-1.58937
C	-0.84320	-1.71422	-0.38700
H	-1.33359	-1.47422	0.56079
H	-0.31132	-2.65710	-0.22204
C	-1.88855	-1.91178	-1.48773
H	-2.48712	-1.00106	-1.61033
H	-1.37924	-2.08416	-2.44302
C	-2.82564	-3.08083	-1.18604
H	-3.36040	-2.92486	-0.24384
H	-3.57110	-3.20494	-1.97610
H	-2.26787	-4.01860	-1.10150

10.12. $[N_{2,2,1,0}]^+$

Table S16. $[N_{2,2,1,0}]^+$ (SMD). Units in Ångströms. Cartesian axes.

Atom	X	Y	Z
N	-0.56420	0.82849	-0.42803
H	-1.58209	0.72190	-0.41454
C	-0.22581	1.50584	-1.73631
H	-0.71713	2.47755	-1.69146
H	0.85085	1.66824	-1.73840
C	-0.21044	1.70618	0.72940
H	-0.76918	2.63537	0.63582
H	-0.48094	1.19425	1.65077
H	0.85672	1.91186	0.70789
C	-0.01498	-0.57725	-0.28010
H	-0.50339	-1.17870	-1.04477
H	-0.36473	-0.91924	0.69381
C	1.49461	-0.66537	-0.38673
H	1.77904	-1.70716	-0.22286
H	1.85870	-0.37574	-1.37394
H	2.00029	-0.06252	0.36934
C	-0.69047	0.71828	-2.94515
H	-0.53112	1.33064	-3.83517
H	-0.13481	-0.21131	-3.07679
H	-1.75790	0.48830	-2.88437

10.13. $[C_4Py]^+$

Table S17. $[C_4Py]^+$ (SMD). Units in Ångströms. Cartesian axes.

Atom	X	Y	Z
C	2.57954	-0.50713	0.75061
C	3.22534	0.70695	0.63062
C	2.61718	1.73284	-0.08778
C	1.37116	1.51248	-0.66824
C	0.76613	0.28044	-0.52035
H	2.99302	-1.34521	1.29347
H	4.19058	0.83833	1.09993
H	3.10719	2.69254	-0.19219
H	0.86373	2.28422	-1.23040
H	-0.19934	0.04260	-0.94414
C	0.73153	-2.04127	0.26462
H	1.01095	-2.46826	1.22701
H	-0.34565	-1.88080	0.25452
C	1.17560	-2.93041	-0.89216
H	2.26619	-3.02898	-0.86963
H	0.91311	-2.44438	-1.83788
C	0.52376	-4.31221	-0.81644
H	0.78963	-4.78572	0.13521
H	-0.56592	-4.19784	-0.81481
C	0.94401	-5.21519	-1.97546
H	2.02771	-5.36842	-1.98338
H	0.46839	-6.19697	-1.90178
H	0.66129	-4.77802	-2.93824
N	1.37115	-0.70111	0.18112

10.14. $[P_{6,6,6,14}]^+$

Table S18. $[P_{6,6,6,14}]^+$ (SMD). Units in Ångströms. Cartesian axes.

Atom	X	Y	Z
P	-3.22709	0.23660	0.01323
C	-3.16545	1.86418	0.82394
H	-4.13850	2.00890	1.30276
H	-2.42118	1.77939	1.62191
C	-2.83555	3.03170	-0.11683
H	-3.59576	3.10184	-0.90179
H	-1.87838	2.84844	-0.61653
C	-1.64872	-0.10433	-0.82447
H	-1.59474	0.57953	-1.67713
H	-1.72827	-1.11881	-1.22652
C	-0.41128	0.03827	0.07272
H	-0.49959	-0.62381	0.94061
H	-0.34978	1.06170	0.45700
C	0.87442	-0.29358	-0.69150
H	0.82272	-1.32873	-1.05100
H	0.93692	0.34214	-1.58349
C	2.13777	-0.10759	0.15301
H	2.06344	-0.72227	1.05928
H	2.19544	0.93497	0.49140
C	-3.51781	-1.04558	1.27139
H	-3.39351	-2.00852	0.76664
H	-2.70424	-0.95248	1.99704
C	-4.88623	-0.95791	1.96194
H	-5.00312	0.02422	2.43209
H	-5.68235	-1.04923	1.21565
C	-4.57018	0.22273	-1.21392
H	-5.47382	0.54851	-0.68982
H	-4.32427	0.99593	-1.94780
C	-4.78681	-1.13482	-1.89758
H	-5.02342	-1.89439	-1.14503
H	-3.86303	-1.45302	-2.39217
C	3.42216	-0.46880	-0.59893
H	3.36992	-1.51780	-0.91814
H	3.48300	0.12866	-1.51787
C	4.69465	-0.25494	0.22598
H	4.75563	0.79823	0.52986
H	4.62810	-0.83863	1.15343
C	5.97455	-0.64077	-0.52173
H	6.03455	-0.06665	-1.45563
H	5.91612	-1.69718	-0.81482
C	7.25193	-0.41383	0.29224
H	7.18724	-0.97787	1.23198
H	7.31799	0.64521	0.57401
C	8.52787	-0.81965	-0.45173
H	8.59074	-0.25969	-1.39402
H	8.46148	-1.87985	-0.72913

C	9.80782	-0.59039	0.35762
H	9.74030	-1.14185	1.30459
H	9.88107	0.47173	0.62565
C	11.08067	-1.01388	-0.38183
H	11.14776	-0.46472	-1.33017
H	11.00663	-2.07661	-0.64741
C	12.36188	-0.78486	0.42535
H	12.29218	-1.32791	1.37719
H	12.44211	0.27911	0.68459
C	13.63363	-1.22078	-0.30920
H	13.70334	-0.67959	-1.26097
H	13.55437	-2.28460	-0.56543
C	14.90745	-0.98619	0.50568
H	14.87830	-1.53821	1.45132
H	15.79910	-1.30988	-0.04036
H	15.03250	0.07520	0.74569
C	-5.05678	-2.05023	3.02242
H	-4.92997	-3.03339	2.55236
H	-4.25803	-1.95667	3.76861
C	-6.41784	-1.98948	3.72074
H	-6.54570	-1.00000	4.17873
H	-7.21444	-2.08728	2.97175
C	-6.60000	-3.06723	4.79381
H	-5.80447	-2.96860	5.54265
H	-6.47239	-4.05639	4.33706
C	-7.96332	-2.99518	5.48485
H	-8.77846	-3.12957	4.76574
H	-8.06550	-3.76963	6.25120
H	-8.10751	-2.02456	5.97149
C	-2.76260	4.36071	0.64179
H	-3.71963	4.54160	1.14668
H	-2.00435	4.28335	1.43096
C	-2.43247	5.54753	-0.26716
H	-1.47642	5.36160	-0.77362
H	-3.19079	5.62152	-1.05740
C	-2.35428	6.88078	0.48282
H	-1.60025	6.80389	1.27577
H	-3.31134	7.06793	0.98511
C	-2.01651	8.06126	-0.43013
H	-2.76955	8.18108	-1.21644
H	-1.96873	8.99992	0.13042
H	-1.04746	7.91670	-0.91977
C	-5.91791	-1.07198	-2.92902
H	-6.83999	-0.74284	-2.43411
H	-5.67838	-0.30931	-3.68032
C	-6.16247	-2.41383	-3.62413
H	-5.23401	-2.74635	-4.10624
H	-6.40756	-3.17316	-2.87021
C	-7.28110	-2.36181	-4.66948
H	-7.03485	-1.60363	-5.42294

H	-8.20912	-2.02901	-4.18867
C	-7.51568	-3.70821	-5.35732
H	-7.79217	-4.47934	-4.63033
H	-8.31824	-3.64680	-6.09864
H	-6.61201	-4.04924	-5.87381

10.15. PC

Table S19. PC (SMD). Units in Ångströms. Cartesian axes.

Atom	X	Y	Z
C	-0.58505	1.31217	0.18032
O	0.73612	1.06507	-0.36856
C	1.13695	-0.17055	-0.01760
C	-1.10002	-0.09466	0.49776
H	-0.47305	1.93167	1.07040
H	-1.17779	1.82882	-0.57143
H	-1.56924	-0.14243	1.47836
O	0.15326	-0.84859	0.59553
O	2.23646	-0.60733	-0.22628
C	-1.97939	-0.70375	-0.57232
H	-2.20326	-1.74662	-0.33849
H	-2.92069	-0.14977	-0.62021
H	-1.49766	-0.65423	-1.55317

10.16. MeCN

Table S20. MeCN (SMD). Units in Ångströms. Cartesian axes.

Atom	X	Y	Z
N	0.00000	0.00000	1.43053
H	0.88991	-0.51379	-1.54332
H	0.00000	1.02758	-1.54332
H	-0.88991	-0.51379	-1.54332
C	0.00000	0.00000	0.27665
C	0.00000	0.00000	-1.17394

10.17. Water

Table S21. Water (SMD). Units in Ångströms. Cartesian axes.

Atom	X	Y	Z
O	0.00000	0.11837	0.00000
H	0.76233	-0.47349	0.00000
H	-0.76233	-0.47350	0.00000

10.18. EtOH

Table S22. EtOH (SMD). Units in Ångströms. Cartesian axes.

Atom	X	Y	Z
O	1.16476	-0.39617	0.00003
H	1.99350	0.09808	-0.00018
C	0.07532	0.54707	0.00001
H	0.14224	1.18766	0.88720
H	0.14227	1.18766	-0.88717
C	-1.22741	-0.22372	-0.00001
H	-1.30560	-0.85759	0.88823
H	-2.07232	0.47098	0.00001
H	-1.30560	-0.85754	-0.88829

10.19. Imidazole

Table S23. Imidazole (SMD). Units in Ångströms. Cartesian axes.

Atom	X	Y	Z
C	0.62159	0.97548	0.00004
C	1.13963	-0.29395	0.00001
H	1.08052	1.94989	0.00009
H	2.17711	-0.58995	0.00001
C	-1.00054	-0.52592	-0.00003
N	0.11889	-1.22542	-0.00004
N	-0.74517	0.80877	0.00002
H	-2.00256	-0.92467	-0.00006
H	-1.43514	1.54760	0.00004

11. References

1. J. M. Seymour, E. Gousseva, A. I. Large, C. J. Clarke, P. Licence, R. M. Fogarty, D. A. Duncan, P. Ferrer, F. Venturini, R. A. Bennett, R. G. Palgrave and K. R. J. Lovelock, *Phys. Chem. Chem. Phys.*, 2021, **23**, 20957-20973.
2. R. M. Fogarty, R. G. Palgrave, R. A. Bourne, K. Handrup, I. J. Villar-Garcia, D. J. Payne, P. A. Hunt and K. R. J. Lovelock, *Phys. Chem. Chem. Phys.*, 2019, **21**, 18893-18910.
3. V. S. Bernales, A. V. Marenich, R. Contreras, C. J. Cramer and D. G. Truhlar, *J. Phys. Chem. B*, 2012, **116**, 9122-9129.
4. K. Hernández-Burgos, S. E. Burkhardt, G. G. Rodríguez-Calero, R. G. Hennig and H. D. Abruña, *J. Phys. Chem. C*, 2014, **118**, 6046-6051.
5. C. Reichardt and T. Welton, *Solvents and Solvent Effects in Organic Chemistry*, Wiley, Weinheim, 4th edn., 2011.
6. W. M. Haynes, ed., *"Physical Constants of Organic Compounds" in CRC Handbook of Chemistry and Physics 96th Edition (Internet Version)*, CRC Press/Taylor and Francis, Boca Raton, 2015.
7. A. W. Adamson and A. P. Gast, *Physical chemistry of surfaces*, Wiley, New York, 6th edn., 1997.
8. A. M. Zissimos, M. H. Abraham, A. Klamt, F. Eckert and J. Wood, *Journal of Chemical Information and Computer Sciences*, 2002, **42**, 1320-1331.
9. R. S. Mulliken, *J. Chem. Phys.*, 1955, **23**, 1833-1840.
10. T. Lu and F. W. Chen, *J. Comput. Chem.*, 2012, **33**, 580-592.
11. A. D. Becke, *Phys. Rev. A*, 1988, **38**, 3098-3100.
12. C. T. Lee, W. T. Yang and R. G. Parr, *Phys. Rev. B*, 1988, **37**, 785-789.
13. M. J. Frisch, G. W. Trucks, H. B. Schlegel, G. E. Scuseria, M. A. Robb, J. R. Cheeseman, G. Scalmani, V. Barone, B. Mennucci, G. A. Petersson, H. Nakatsuji, M. Caricato, X. Li, H. P. Hratchian, A. F. Izmaylov, J. Bloino, G. Zheng, J. L. Sonnenberg, M. Hada, M. Ehara, K. Toyota, R. Fukuda, J. Hasegawa, M. Ishida, T. Nakajima, Y. Honda, O. Kitao, H. Nakai, T. Vreven, J. J. A. Montgomery, J. E. Peralta, F. Ogliaro, M. Bearpark, J. J. Heyd, E. Brothers, K. N. Kudin, V. N. Staroverov, R. Kobayashi, J. Normand, K. Raghavachari, A. Rendell, J. C. Burant, S. S. Iyengar, J. Tomasi, M. Cossi, N. Rega, J. M. Millam, M. Klene, J. E. Knox, J. B. Cross, V. Bakken, C. Adamo, J. Jaramillo, R. Gomperts, R. E. Stratmann, O. Yazyev, A. J. Austin, R. Cammi, C. Pomelli, J. W. Ochterski, R. L. Martin, K. Morokuma, V. G. Zakrzewski, G. A. Voth, P. Salvador, J. J. Dannenberg, S. Dapprich, A. D. Daniels, Ö. Farkas, J. B. Foresman, J. V. Ortiz, J. Cioslowski and D. J. Fox, *Journal*, 2009.
14. S. Grimme, S. Ehrlich and L. Goerigk, *J. Comput. Chem.*, 2011, **32**, 1456-1465.
15. A. D. Becke and E. R. Johnson, *J. Chem. Phys.*, 2005, **123**, 154101.
16. A. D. Becke and E. R. Johnson, *J. Chem. Phys.*, 2006, **124**, 014104.
17. S. Grimme, J. Antony, S. Ehrlich and H. Krieg, *J. Chem. Phys.*, 2010, **132**, 154104.
18. C. Ehlert, M. Holzweber, A. Lippitz, W. E. S. Unger and P. Saalfrank, *Phys. Chem. Chem. Phys.*, 2016, **18**, 8654-8661.
19. I. J. Villar-Garcia, E. F. Smith, A. W. Taylor, F. L. Qiu, K. R. J. Lovelock, R. G. Jones and P. Licence, *Phys. Chem. Chem. Phys.*, 2011, **13**, 2797-2808.
20. M. J. Thomason, C. R. Seabourne, B. M. Sattelle, G. A. Hembury, J. S. Stevens, A. J. Scott, E. F. Aziz and S. L. M. Schroeder, *Faraday Discuss.*, 2015, **179**, 269-289.
21. D. Nolting, N. Ottosson, M. Faubel, I. V. Hertel and B. Winter, *J. Am. Chem. Soc.*, 2008, **130**, 8150-8151.
22. R. M. Fogarty, R. P. Matthews, C. R. Ashworth, A. Brandt-Talbot, R. G. Palgrave, R. A. Bourne, T. V. Hoogerstraete, P. A. Hunt and K. R. J. Lovelock, *J. Chem. Phys.*, 2018, **148**, 193817.
23. R. M. Fogarty, R. P. Matthews, M. T. Clough, C. R. Ashworth, A. Brandt-Talbot, P. J. Corbett, R. G. Palgrave, R. A. Bourne, T. W. Chamberlain, T. Vander Hoogerstraete, P. B. J. Thompson, P. A. Hunt, N. A. Besley and K. R. J. Lovelock, *Phys. Chem. Chem. Phys.*, 2017, **19**, 31156-31167.